The Canadian Mineralogist
Vol. 58, pp. 19-43 (2020)
DOI: 10.3749/canmin.1900070

FROM STRUCTURE TOPOLOGY TO CHEMICAL COMPOSITION. XXVII. REVISION OF THE CRYSTAL CHEMISTRY OF THE PERRAULTITE-TYPE MINERALS OF THE SEIDOZERITE SUPERGROUP: JINSHAJIANGITE, SURKHOBITE, AND BOBSHANNONITE

Elena SOKOLOVA[§] and Frank C. HAWTHORNE

Department of Geological Sciences, University of Manitoba, Winnipeg, Manitoba, R3T 2N2, Canada

Fernando CÁMARA

Dipartimento di Scienze della Terra "Ardito Desio", Università degli Studi di Milano, Via Mangiagalli 34, 20133, Milano, Italy

Giancarlo DELLA VENTURA

Dipartimento di Scienze, Università di Roma Tre, Largo S. Leonardo Murialdo 1, I-00146 Roma, Italy
INFN-Laboratori Nazionali di Frascati (Roma), Italy

Yulia A. UVAROVA

CSIRO Mineral Resources, ARRC, 29 Dick Perry Avenue, Kensington, Western Australia 6151 Australia

Abstract

The crystal structures of the three perraultite-type minerals (bafertisite group, seidozerite supergroup)—jinshajiangite from Norra Kärr, Sweden, ideally $NaBaFe^{2+}_4Ti_2(Si_2O_7)_2O_2(OH)_2F$, $Z = 4$; surkhobite (holotype) from the Darai-Pioz massif, Tajikistan, ideally $NaBaMn_4Ti_2(Si_2O_7)_2O_2(OH)_2F$, $Z = 4$; and bobshannonite (holotype) from Mont Saint-Hilaire, Canada, ideally $Na_2KBa(Mn_7Na)Nb_4(Si_2O_7)_4O_4(OH)_4O_2$, $Z = 2$—were refined in space group $C\bar{1}$ to $R_1 = 2.73$, 2.85, and 2.02% on the basis of 2746, 2657, and 4963 unique reflections [$F_o > 4\sigma F_o$], respectively. Refinement was done using data from twinned crystals (jinshajiangite: three twin components; surkhobite and bobshannonite: two twin components). The parameters of a *C*-centered triclinic unit cell are as follows: jinshajiangite: $a = 10.720(5)$, $b = 13.823(7)$, $c = 11.044(6)$ Å, $\alpha = 108.222(6)$, $\beta = 99.28(1)$, $\gamma = 89.989(6)°$, $V = 1532.0(2.2)$ Å^3; surkhobite: $a = 10.728(6)$, $b = 13.845(8)$, $c = 11.072(6)$ Å, $\alpha = 108.185(6)$, $\beta = 99.219(5)$, $\gamma = 90.001(8)°$, $V = 1540.0(2.5)$ Å^3; and bobshannonite: $a = 10.831(7)$, $b = 13.903(9)$, $c = 11.149(8)$ Å, $\alpha = 108.145(6)$, $\beta = 99.215(9)$, $\gamma = 90.007(7)°$, $V = 1572.6(3.2)$ Å^3. New electron microprobe data are reported for the holotype surkhobite and new IR data for jinshajiangite. In the perraultite-type structure (structure type B1BG, B – basic, BG – bafertisite group), there is one type of TS (Titanium-Silicate) block and one type of **I** (Intermediate) block; they alternate along **c**. The TS block consists of HOH sheets (H-heteropolyhedral, O-octahedral). In the O sheet, the ideal composition of the five $^{[6]}M^O$ sites is Fe^{2+}_4 *apfu* (jinshajiangite), Mn_4 *apfu* (surkhobite), and (Mn_7Na) (bobshannonite). There is no order of Fe^{2+} and Mn in the O sheet. In the H sheet, the ideal composition of the two $^{[6]}M^H$ sites is Ti_2 *apfu* (jinshajiangite, surkhobite) and Nb_4 *apfu* (bobshannonite). The four $^{[4]}Si$ sites are occupied solely by Si. The M^H octahedra and Si_2O_7 groups constitute the H sheet. The TS blocks link *via* common vertices of M^H octahedra. The **I** block contains $A^P(1,2)$ and $B^P(1,2)$ cation sites. In the **I** block of jinshajiangite and surkhobite, the $A^P(1)$ site is occupied by Ba and the $A^P(2)$ site by K > Ba; the ideal composition of the two $A^P(1,2)$ sites is Ba *apfu*. In the **I** block of bobshannonite, Ba and K are ordered at the $A^P(1)$ and $A^P(2)$ sites, Ba:K ~ 1:1 , ideally BaK *apfu*. The two $B^P(1,2)$ sites are each occupied by Na > Ca, ideally Na *apfu* (jinshajiangite, surkhobite) and solely by Na, ideally Na_2 *apfu* (bobshannonite). There is no order of Na and Ca at the $B^P(1,2)$ sites in jinshajiangite and surkhobite [currently defined as a Ca-ordered analogue of perraultite, ideally $NaBaMn_4Ti_2(Si_2O_7)_2O_2(OH)_2F$, $Z = 4$]. The ideal formulae of surkhobite, $KBa_3Ca_2Na_2Mn_{16}Ti_8(Si_2O_7)_8O_8(OH)_4(F,O,OH)_8$ (current IMA formula) and of bobshannonite, $Na_2KBa(Mn,Na)_8(Nb,Ti)_4(Si_2O_7)_4O_4(OH)_4(O,F)_2$ (current IMA formula) have been revised as follows: $NaBaMn_4Ti_2(Si_2O_7)_2O_2(OH)_2F$, $Z = 4$ (surkhobite) and $Na_2KBa(Mn_7Na)Nb_4(Si_2O_7)_4O_4(OH)_4O_2$, $Z = 2$ (bobshannonite). The revised ideal formula of surkhobite is identical to the ideal formula of perraultite and hence surkhobite should be discredited.

[§] *Corresponding author e-mail address*: Elena.sokolova@umanitoba.ca

Keywords: perraultite, jinshajiangite, surkhobite, bobshannonite, bafertisite group, seidozerite supergroup, TS block, crystal-structure refinement, IR spectroscopy, electron-microprobe analysis.

INTRODUCTION

Perraultite, ideally $NaBaMn_4Ti_2(Si_2O_7)_2O_2(OH)_2F$; jinshajiangite, ideally $NaBaFe^{2+}{}_4Ti_2(Si_2O_7)_2O_2(OH)_2F$; surkhobite, $KBa_3Ca_2Na_2Mn_{16}Ti_8(Si_2O_7)_8O_8(OH)_4(F,O,OH)_8$ (current IMA formula); and bobshannonite, ideally $Na_2KBa(Mn,Na)_8(Nb,Ti)_4(Si_2O_7)_4O_4(OH)_4(O,F)_2$ (current IMA formula) are bafertisite-group minerals of the seidozerite supergroup. They belong to the structure type of perraultite (Yamnova *et al*. 1998); later in this paper we will call them perraultite-type minerals [the ideal formulae of perraultite, jinshajiangite, and bobshannonite are in accord with the current nomenclature of the seidozerite supergroup (Sokolova & Cámara 2017)]. There are 47 well-characterized seidozerite-supergroup minerals: 45 minerals including surkhobite (Sokolova & Cámara 2017), plus rinkite-(Y), ideally $Na_2Ca_4YTi(Si_2O_7)_2OF_3$ (Pautov *et al*. 2019) and fluorbarytolamprophyllite, ideally $Na_3(BaK)Ti_3(Si_2O_7)_2O_2F_2$ (Filina *et al*. 2019), which have structures based on a TS-block (TS = Titanium-Silicate). Note that where we say "well-characterized" seidozerite-supergroup minerals, we do not include bykovaite (Khomyakov *et al*. 2005), selivanovaite (Pakhomovsky *et al*. 2018), or shkatulkalite (Men'shikov *et al*. 1996, Zolotarev *et al*. 2018), as these minerals either lack structural data (bykovaite), or there is a lack of agreement between structure-refinement results and chemical composition (shkatulkalite), or poor interpretation of structure-refinement results (selivanovaite). The TS-block consists of HOH sheets (H = heteropolyhedral, O = octahedral) and is characterized by a planar cell based on translation vectors, $\mathbf{t_1}$ and $\mathbf{t_2}$, with $t_1 \sim 5.5$ and $t_2 \sim 7$ Å and $t_1 \wedge t_2$ close to 90°. The seidozerite-supergroup minerals are divided into four groups based on the content of Ti (+ Nb + Zr + Fe^{3+} + Mg + Mn), topology, chemical composition, and stereochemistry of the TS block (Sokolova 2006, 2010, Sokolova & Cámara 2013, Sokolova & Cámara 2017). In the rinkite, bafertisite, lamprophyllite, and murmanite groups, Ti (+ Nb + Zr + Fe^{3+} + Mg + Mn) = 1, 2, 3, and 4 *apfu* (atoms per formula unit). Sokolova & Cámara (2013) introduced the concept of *basic* and *derivative structures* for TS-block minerals. A *basic structure* has the following four characteristics: (1) there is only one type of TS block; (2) the two H sheets of the TS block are identical; (3) there is only one type of **I** block or it is absent; (4) there is only one type of self-linkage of TS blocks. Basic structures obey the general structural principles of Sokolova (2006). A *derivative structure* has one or more of the three following characteristics: (1) there is more than one type of TS block; (2) there is more than one type of **I** block; (3) there is more than one type of self-linkage of TS blocks. A derivative structure is related to two or more basic structures of the same Group; it can be derived by adding these structures *via* sharing the central O sheet of the TS blocks of adjacent structural fragments which represent basic structures. There are five seidozerite-supergroup minerals with derivative structures: cámaraite, ideally $NaBa_3Fe^{2+}{}_8Ti_4(Si_2O_7)_4O_4(OH)_4F_3$ (Sokolova *et al*. 2009b, Cámara *et al*. 2009); bornemanite, ideally $Na_6BaTi_2Nb(Si_2O_7)_2(PO_4)O_2(OH)F$ (Men'shikov *et al*. 1975, Cámara & Sokolova 2007); saamite, ideally $Na_3BaTi_2Nb(Si_2O_7)_2O_2(OH)_2(H_2O)_2$ (Cámara *et al*. 2014); kazanskyite, ideally $Na_3BaTi_2Nb(Si_2O_7)_2O_2(OH)_2(H_2O)_4$ (Cámara *et al*. 2012); and nechelyustovite, ideally $Na_6Ba_2Ti_4Nb_2(Si_2O_7)_4O_4(OH)_4(H_2O)_6$ (Nèmeth *et al*. 2009, Cámara & Sokolova 2009).

Perraultite and the perraultite-type minerals jinshajiangite, surkhobite, and bobshannonite have basic structures characterized by doubled t_1 and t_2 unit-cell parameters; previous structure information for the perraultite-type minerals is given in Table 1. In this paper, we consider data where structure-refinement (solution) results are supported by a corresponding chemical analysis (except for the first chemical analysis in the description of a new mineral species where structure was not known at that time) and *vice versa*. Hence, we do not consider data from Lykova *et al*. (2010) (solely chemical analysis of jinshajiangite) or Rastsvetaeva *et al*. (2008a) (solely crystal-structure refinement of jinshajiangite).

Jinshajiangite, $(Na,K)_5(Ba,Ca)_4(Fe^{2+},Mn)_{15}(Ti,Fe^{3+},Nb)_8(SiO_4)_{15}(F,O,OH)_{10}$, $Z = 2$, from the Jinshajiang River, Sichuan Province, China, was described as a new mineral by Hong & Fu (1982). Chao (1991) described perraultite, ideally $Na_2KBa(Ti,Nb)_4Mn_8Si_8O_{32}(OH,F,H_2O)_7$, $Z = 4$, from Mont Saint-Hilaire, Québec, Canada, and suggested that perraultite is isotypic with jinshajiangite. Yamnova *et al*. (1998) solved the crystal structure of perraultite from the Oktyabr'skii (formerly Mariupol'skii) massif in the coastal region of the Azov Sea (Donetsk region, Ukraine) and gave the following information: monoclinic, space group *C*2 (Table 1), and generalized crystal-chemical formula $(Na,Ca)_2(Ba,K)_2(Mn,Fe)_8[(Ti,Nb)_4O_4(OH)_2Si_8O_{28}](OH,F)_4$, $Z = 4$. A descrip-

TABLE 1. PREVIOUS STRUCTURAL DATA FOR THE PERRAULTITE-TYPE MINERALS (STRUCTURE TYPE B1BG)*

Mineral	Ideal structural formula**								*a* (Å) α (°)	*b* (Å) β (°)	*c* (Å) γ (°)	Sp. gr.	*Z*	R_1 (%)	Ref.
	A^P	B^P	$M^O{}_4$	$M^H{}_2$	$(Si_2O_7)_2$	$(X^O{}_M)_2$	$(X^O{}_A)_2$	$X^P{}_M$							
									Monoclinic						
Perraultite	Ba	Na	Mn_4	Ti_2	$(Si_2O_7)_2$	O_2	$(OH)_2$	F	10.731	13.841	20.845	*C*2	8	6.2	(1)
									90	95.06	90				
Surkhobite_2003	$(Ba,K)_2$	$(Ca,Na)_2$	$(Fe,Mn,Na)_8$	$(Ti,Nb,Zr)_4$	$(Si_2O_7)_4$	O_4	$[F_3(OH)]$	$(F,OH,O)_2$	10.723	13.826	20.791	*C*2	4	4.7	(2)
									90	95.00	90				
Surkhobite_2008	K Ba_3	Ca_2 Na_2	Mn_{16}	Ti_8	$(Si_2O_7)_8$	O_8	$F_6(OH)_2$	$F_2(OH)_2$	10.723	13.826	20.791	*C*2	2	4.3	(3)
									90	95.00	90				
Jinshajiangite_2009	Ba	Na	$Fe^{2+}{}_4$	Ti_2	$(Si_2O_7)_2$	O_2	$(OH)_2$	F	10.6785	13.786	20.700	*C*2/*m*	8	5.69	(4)
									90	94.937	90				
									Triclinic						
Bobshannonite***	K Ba	Na_2	$(Mn,Na)_8$	$(Nb,Ti)_4$	$(Si_2O_7)_4$	O_4	$(OH)_4$	$(O,F)_2$	10.839	13.912	20.98	$C\bar{1}$	4	2.55	(5)
									89.99	95.02	89.998				
									8.818	8.818	20.982	$P\bar{1}$	2		
									93.09	93.11	104.16				
Jinshajiangite_2016***	Ba	Na	$Fe^{2+}{}_4$	Ti_2	$(Si_2O_7)_2$	O_2	$(OH)_2$	F	10.7059	13.7992	20.760	$C\bar{1}$	8	3.13	(6)
									90.008	94.972	89.984				
									8.7314	8.7338	20.760	$P\bar{1}$	4		
									93.051	93.039	104.389				
Jinshajiangite_2018***	Ba	Na	$Fe^{2+}{}_4$	Ti_2	$(Si_2O_7)_2$	O_2	$(OH)_2$	F	8.7331	8.7336	11.0404	$P\bar{1}$	2	4.1	(7)
									81.477	110.184	104.384				
									10.7092	13.8023	11.0404	$C\bar{1}$	4		(8)
									108.187	108.187	90.024				

* Structure type (B1BG: B - basic, BG – bafertisite group) and ideal structural formulae for perraultite, jinshajiangite, and bobshannonite are from Sokolova & Cámara (2017); surkhobite_2003 has "crystallochemical formula"; formulae are per $(Si_2O_7)_2$, except for surkhobite_2003 and bobshannonite: per $(Si_2O_7)_4$ and surkhobite_2008: per $(Si_2O_7)_8$.

** Atom labelling: M^H = cations of the H sheet, M^O = cations of the O sheet, A^P and B^P = cations at the peripheral (*P*) sites; $X^O{}_M$ = common anions for three M^O octahedra of the O sheet and one M^H octahedron of the H sheet; $X^O{}_A$ = common anions for three M^O octahedra of the O sheet; $X^P{}_M$ = bridging anion between two M^H octahedra (Sokolova 2006).

*** For bobshannonite and jinshajiangite_2016, the second line reports a reduced cell; for jinshajiangite_2018, the unit-cell parameters corresponding to the space group $C\bar{1}$ have been calculated using the transformation matrix $(\bar{1}\bar{1}0, \bar{1}10, 00\bar{1})(P\bar{1} \rightarrow C\bar{1})$.

References: (1) Yamnova *et al.* (1998); (2) Rozenberg *et al.* (2003); (3) Rastsvetaeva *et al.* (2008b); (4) Sokolova *et al.* (2009a); (5) Sokolova *et al.* (2015); (6) Cámara *et al.* (2016b); (7) Jin *et al.* (2018); (8) this work.

tion of perraultite from this locality was given by Pekov *et al*. (1999). Sokolova (2006) considered perraultite as a TS-block mineral and wrote its ideal formula as $NaBaMn_4Ti_2(Si_2O_7)_2O_2(OH)_2F$, $Z = 8$.

Eskova *et al*. (2003) described surkhobite as a Ca-analogue of jinshajiangite from the Darai-Pioz massif, Tajikistan; they reported the chemical analysis (bulk chemistry) (Table 2) and the simplified formula $(Ca,Na)(Ba,K)(Fe^{2+},Mn)_4Ti_2(Si_2O_7)_2O_2(F,OH,O)_3$, $Z = 8$ (Table 1). Using the atom coordinates of perraultite from Yamnova *et al*. (1998) (space group *C*2), Rozenberg *et al*. (2003) refined the crystal structure of surkhobite and reported dominant Ca over Na in the "zeolite channels" of the structure. Eskova *et al*. (2003) stated that the "major difference of surkhobite from perraultite and jinshajiangite was prevalence of Ca over Na in the zeolite channels, and from perraultite - plus prevalence of iron over manganese". Rozenberg *et al*. (2003) wrote the structural formula of surkhobite as follows: $\{[Ca_{1.2}Na_{0.8}][Ba_{1.65}K_{0.35}]\}\{[Fe_4][Mn_{3.7}Na_{0.3}]\}\{[Ti_{3.2}(Zr,Nb)_{0.8}]O_4F(OH,O)][Si_2O_7]_4\}\{[F_3(OH)]\}$, $Z = 4$. Attempts to write an ideal formula for surkhobite [based on the structural data and structural formula of surkhobite by Rozenberg *et al*. (2003)] resulted in an ideal formula of the form $CaBaFe^{2+}{}_4Ti_2(Si_2O_7)_2O_2(F,OH)_2F$, $Z = 8$ (Sokolova 2006). Sokolova (2006) noted that the latter formula of surkhobite was doubtful, as it had an excess charge of +1. She suggested that the probable formula of surkhobite was $NaBaFe^{2+}{}_4Ti_2(Si_2O_7)_2O_2(OH)F_2$ and pointed out that the chemical composition of surkhobite needed to be reinvestigated, and the chemical formula needed to be revised. Sokolova used the holotype specimen of surkhobite from the Fersman Mineralogical Museum, Moscow, Russia (registration # 2882/1) for the microprobe analysis [Table 2, analysis (8); see experimental details below] and reported major differences between the EMPA data of 2006 and those reported for surkhobite by Eskova *et al*. (2003), *i.e*., a lower content both of Ca and F: CaO 2.48 *versus* 4.74 and F 2.65 *versus* 4.06 wt.%, respectively (Table 2). Sokolova wrote the ideal formula for the holotype surkhobite as $NaBaTi_2Fe^{2+}{}_4(Si_2O_7)_2O_2(OH)_2F$ and pointed out that (1) the latter formula corresponds to the simplified formula of jinshajiangite of Hong & Fu (1982) (see above), and (2) thus surkhobite and jinshajiangite are the same species; jinshajiangite (IMA 81-061) had been described in 1982, it had priority over surkhobite, and hence surkhobite was not a valid mineral species and needed to be discredited. Based on Nomenclature Voting Proposal 06-E, surkhobite, species and mineral name, were discredited by the CNMNC-IMA: IMA No. 06-E. In 2006, we collected single-crystal X-ray data for the holotype surkhobite, but the refinement in space group *C*2 was unstable. Rastsvetaeva *et al*. (2008b) revalidated surkhobite (IMA-07-A) and redefined it with the new formula $(Ba,K)_2CaNa(Mn,Fe^{2+},Fe^{3+})_8Ti_4(Si_2O_7)_4O_4(F,OH,O)_6$, $Z = 4$ and a simplified formula $KBa_3Ca_2Na_2Mn_{16}Ti_8(Si_2O_7)_8O_8(OH)_4(F,O,OH)_8$, $Z = 2$ (current IMA formula). Rastsvetaeva *et al*. (2008b) called surkhobite "a Mn-dominant analogue of jinshajiangite" which "differs from perraultite in that Ca is ordered onto and is dominant in the site A(6)". To summarize information given in quotes in the latter sentence, Rastsvetaeva *et al*. (2008b) redefined surkhobite as a Ca-ordered analogue of perraultite. Rastsvetaeva *et al*. (2008b) reported a new microprobe analysis of the holotype surkhobite from the Fersman Mineralogical Museum (Table 2, analysis (9)] and Fe^{3+}/Fe^{2+} atomic ratio based on Mössbauer-spectroscopy results and re-refined the crystal structure using the single-crystal X-ray data of Rozenberg *et al*. (2003) (Table 1).

Sokolova *et al*. (2009a) refined the crystal structure of jinshajiangite from Norra Kärr, Jönköping province, Sweden, in space group *C*2/*m*, determined Fe^{2+}/Fe^{3+} atomic ratio by Mössbauer spectroscopy, and wrote its ideal formula as $BaNaTi_2Fe^{2+}{}_4(Si_2O_7)_2O_2(OH)_2F$, $Z = 8$, in accord with Sokolova (2006). Sokolova *et al*. (2015) described bobshannonite, a Nb-analogue of perraultite (Table 1), and refined its crystal structure as triclinic from a twinned crystal (two components) in space group $C\bar{1}$. They reported a reduced unit cell, space group $P\bar{1}$ (Table 1) related to the $C\bar{1}$ unit cell by the transformation matrix (½-½0 ½½0 001). Sokolova *et al*. (2015) chose the unconventional space group $C\bar{1}$ to make comparison with the TS-block structures more straightforward: the TS-block structures are characterized by two minimal translations, $t_1 \sim 5.4$ and $t_2 \sim 7$ Å. Following the work of Sokolova *et al*. (2015) on bobshannonite, the crystal structures of the three bafertisite-group minerals related to bobshannonite were revisited and refined in space group $C\bar{1}$: jinshajiangite (Table 1, Cámara *et al*. 2016b); bafertisite, ideally $Ba_2Fe^{2+}{}_4Ti_2(Si_2O_7)_2O_2(OH)_2F_2$ (Cámara *et al*. 2016a); and hejtmanite (holotype), ideally $Ba_2Mn_4Ti_2(Si_2O_7)_2O_2(OH)_2F_2$ (Sokolova *et al*. 2016). We also re-collected single-crystal X-ray data for the holotype surkhobite and attempted to refine the structure in space group $C\bar{1}$ using the atom coordinates of bobshannonite; the refinement was unstable. Jin *et al*. (2018) studied jinshajiangite from the type locality, the Jinshajiang River area in Sichuan Province, China, by TEM (transmission electron microscopy) and Mössbauer spectroscopy and refined its crystal structure in space group $P\bar{1}$, with $c \sim 11$ Å compared to $c \sim 21$ Å in previous refinements of jinshajiangite (unit-cell parameters are given in Table 1). Based on the TEM data and precession photographs, Jin *et al*. (2018) reported four types of twinning for the crystal structure of jinshajiangite. They stated that (1) the basic topology of the new $P\bar{1}$ structure is analogous to the previously proposed $C\bar{1}$ structure of Cámara *et al*. (2016b), except there is only one type of TS block and one type of **I** block in the structure [instead of two types, Cámara *et al*. (2016b)]. Jin *et al*. (2018) suggested that: (1) all minerals with the perraultite-type structure, jinshajiangite itself plus perraultite, surkhobite, and bobshannonite, should have the same $P\bar{1}$ structure as jinshajiangite with $\sim$10 Å d_{001} spacing, *i.e*., with $c \sim 11$ Å instead of the previously reported $c \sim 21$ Å (Table 1); and (2) all previously proposed monoclinic space groups were pseudosymmetry generated by nanoscale polysynthetic twinning on the (001) composition plane. Jin *et al*. (2018) refined the crystal structure of jinshajiangite using the reduced unit cell (space group $P\bar{1}$) based on the two diagonals of the planar cell based on translation vectors $\mathbf{t_1}$ and $\mathbf{t_2}$: $\mathbf{a}_{\text{jin}} = -\mathbf{t_1} - \mathbf{t_2}$ and $\mathbf{b}_{\text{jin}} = -\mathbf{t_1} + \mathbf{t_2}$, whereas the 47 TS-block minerals of the seidozerite supergroup have unit cells based on translation vectors $\mathbf{t_1}$ and $\mathbf{t_2}$ (see above). Such a description of the crystal structure of jinshajiangite complicates comparison of jinshajiangite to perraultite-type and other TS-block structures.

Here, we report new microprobe data and new single-crystal data for holotype surkhobite from the Darai-Pioz massif, Northern Tajikistan (Fersman Mineralogical Museum, Moscow, Russia; registration # 2882/1) and new infrared data for jinshajiangite from Norra Kärr, Sweden. In this paper, we present structure-refinement results for jinshajiangite, surkhobite (holotype), and bobshannonite (holotype) in space group $C\bar{1}$ for better comparison with other TS-block structures. We report revised ideal formulae for surkhobite and bobshannonite. We consider the crystal chemistry of jinshajiangite, surkhobite, and bobshannonite and question the validity of surkhobite as a valid mineral species.

Description of Samples

In this paper, we report on (1) jinshajiangite from Norra Kärr, Sweden [the single crystal was previously studied by Sokolova *et al*. (2009a)]; (2) bobshannonite (holotype) from Mont Saint-Hilaire, Canada [the single crystal was previously studied by Sokolova *et al*. (2015)]; and (3) surkhobite (holotype sample) from the Darai-Pioz massif, Northern Tajikistan (Fersman Mineralogical Museum, Moscow, Russia, registration # 2882/1).

Chemical Composition

Table 2 gives 10 chemical analyses for the perraultite-type minerals. Analyses 1–7, 9, and 10 are taken from the literature (references are given in the footnote), and analysis 8 for the holotype surkhobite is taken from IMA No. 06-E (experimental details are given below). Analyses 1, 5, 7, and 10 are from the original descriptions of new minerals and analyses 2–4, 6, 8, and 9 are accompanied by structure solution/refinements. Further in the paper, we will refer to Fe^{2+} and Fe^{3+} and we will use Mn instead of Mn^{2+}, as only divalent Mn has so far been reported for TS-block minerals of the seidozerite supergroup.

Electron microprobe analysis of surkhobite

Electron microprobe compositions were obtained from the holotype specimen of surkhobite from the Fersman Mineralogical Museum (registration # 2882/1); a part of it had been used for the crystal-structure refinement in Rozenberg *et al*. (2003). One fragment of the holotype crystal of surkhobite was analyzed with a Cameca SX-100 electron-microprobe operating in wavelength-dispersion mode with an accelerating voltage of 15 kV, a specimen current of 20 nA, a beam size of 10 μm, and count times on peak and background of 20 s except for F with count times of 30 s both on peak and background. The following standards and crystals were used for *K* or *L* X-ray lines: F: topaz; Na: albite; Ba: baryte; Si, Ca: diopside; Fe: fayalite; Mn: spessartine; K: orthoclase; Ti: titanite; Zr: zircon; Nb: $BaNaNbO_4$; Mg: forsterite; Sr: $SrTiO_3$; Al: andalusite; Cs: pollucite. Data were reduced using the φ(ρZ) procedure of Pouchou & Pichoir (1985). The chemical composition of the holotype surkhobite is given in Table 2 (analysis 8) and is the mean of 11 determinations. Analyses 8 and 9 were obtained from the same holotype specimen of surkhobite from the Fersman Mineralogical Museum, hence in this paper, we use the Mössbauer-spectroscopy results of Rastsvetaeva *et al*. (2008b) for the assignment of the Fe^{2+}/Fe^{3+} ratio in our analysis 8.

Note that:

(1) the chemical composition of the holotype perraultite (Table 2 analysis 5, EMPA, 3 points) has a very H_2O high content (3.49 wt.%), which is probably due to non-structural H_2O (*i.e*., present in intergrown phases);
(2) the chemical composition of the holotype surkhobite (Table 2 analysis 8) taken from IMA No. 06-E has a lower content of Ca (2.48 wt.%) and F (2.65 wt.%) compared to the composition of Eskova *et al*. (2003): 4.74 and 4.06 wt.%, respectively (Table 2 analysis 7). In 2006, Sokolova suggested that the

TABLE 2. CHEMICAL ANALYSIS* (wt.%) AND FORMULA UNIT (*apfu*) FOR THE PERRAULTITE-TYPE MINERALS

	Jinshajiangite				Perraultite		Surkhobite			Bobshannonite
	(1)	(2)	(3)	(4)	(5)	(6)	(7)	(8)	(9)	(10)
Locality	Jinshajiang River, China Holotype	Norra Kärr, Sweden	Verkhnee Espe deposit, Kazakhstan	Jinshajiang River, China	Mont Saint-Hilaire, Canada Holotype	Oktyabr'-skii massif, Ukraine	Darai-Pioz Massif, Tajikistan Holotype**	Holotype	Holotype	Mont Saint-Hilaire, Canada Holotype
Ta_2O_5	0.07	n.d.	n.d.	n.d.	n.a.	0.11	0.09	n.d.	n.d.	0.52
Nb_2O_5	1.03	0.12	2.74	1.59	13.35	1.24	1.00	1.45	2.14	19.69
ZrO_2	0.70	0.51	0.22	0.76	0.12	1.09	2.40	1.19	0.34	n.d.
TiO_2	15.90	18.36	16.24	17.06	9.44	17.83	14.00	16.73	16.14	5.50
SiO_2	27.10	27.56	27.41	26.74	27.32	27.72	26.68	27.40	27.17	26.31
Ce_2O_3	0.30	n.a.	n.a.	n.d.	n.a.	n.a.	n.a.	n.a.	n.a.	n.a.
Al_2O_3	0.36	n.d.	0.07	n.d.	0.03	0.03	1.10	0.16	0.02	0.06
Fe_2O_3***	1.64	2.89	2.34	1.16	n.a.	0.75	3.47	2.20	2.11	n.a.
FeO	19.07	23.42	19.00	15.07	1.12	12.06	13.0	14.63	13.92	0.89
BaO	9.80	10.24	10.46	10.24	8.88	10.64	14.45	10.41	11.16	7.92
SrO	0.08	n.d.	n.d.	n.d.	n.a.	0.05	0.06	0.21	0.26	n.d.
ZnO	0	n.d.	0.10	n.d.	n.a.	1.02	n.d.	n.d.	n.d.	1.02
MnO	12.98	5.13	10.19	14.76	31.14	19.28	12.75	14.96	16.32	26.34
CaO	2.94	2.52	1.45	2.09	n.d.	1.48.	4.74	2.48	2.53	n.d.
MgO	0.28	0.44	0.19	0.05	0.06	0.04	n.d.	0.13	0.13	0.06
Cs_2O	0	0.03	n.d.	n.d.	n.a.	n.d	0.27	0.28	n.d	n.d
Rb_2O										0.42
K_2O	2.31	1.95	1.92	2.19	2.68	1.67	1.30	2.03	1.87	2.38
Na_2O	3.15	2.27	2.74	2.33	3.52	2.76	1.57	2.10	2.27	4.05
F	2.66	2.33	2.31	2.31	0.84	2.18	4.06	2.65	2.94	0.70
H_2O****	0.33	2.01	1.96	2.00	3.49	1.79	1.17	1.85	1.17	1.95
O = F	–1.12	–0.98	–0.99	–0.97	–0.35	–0.92	–1.71	–1.12	–1.24	–0.29
Total	99.58	98.80	98.39	97.38	101.64	99.80	100.40	99.74	99.25	97.52

TABLE 2. CONTINUED.

	Jinshajiangite				Perraultite		Surkhobite			Bobshannonite
	(1)	(2)	(3)	(4)	(5)	(6)	(7)	(8)	(9)	(10)
Locality	Jinshajiang River, China Holotype	Norra Kärr, Sweden	Verkhnee Espe deposit, Kazakhstan	Jinshajiang River, China	Mont Saint-Hilaire, Canada Holotype	Oktyabr'-skii massif, Ukraine	Darai-Pioz Massif, Tajikistan Holotype**	Holotype	Holotype	Mont Saint-Hilaire, Canada Holotype
	Formula unit calculated on a basis of 19 (O + F) *apfu* (1–9)									38 (O + F) *apfu*
Ta										0.04
Nb	0.07	0.01	0.18	0.11	0.86	0.08	0.07	0.10	0.14	2.73
Zr	0.05	0.04	0.02	0.06	0.01	0.08	0.17	0.08	0.02	
Ti	1.79	1.99	1.79	1.90	1.01	1.94	1.55	1.82	1.79	1.27
Si	4.06	3.97	4.01	3.96	3.90	4.02	3.93	3.97	4.01	8.08
Ce^{3+}	0.02									
Fe^{3+}	0.19	0.31	0.26	0.13		0.08	0.39	0.24	0.24	
Al	0.06		0.01		0.01	0.01	0.19	0.03		0.02
Ba	0.58	0.58	0.60	0.59	0.50	0.60	0.83	0.59	0.65	0.95
Sr	0.01						0.01	0.02	0.02	
Zn			0.01							0.23
Fe^{2+}	2.39	2.83	2.32	1.87	0.13	1.46	1.60	1.77	1.72	0.23
Mn	1.65	0.63	1.26	1.85	3.77	2.37	1.59	1.83	2.04	6.85
Ca	0.47	0.39	0.23	0.33		0.23	0.75	0.39	0.40	
Mg	0.06	0.10	0.04	0.01	0.01	0.01		0.03	0.03	0.03
Cs							0.02	0.02		
Rb										0.08
K	0.44	0.36	0.36	0.41	0.49	0.31	0.24	0.38	0.35	0.93
Na	0.91	0.64	0.78	0.67	0.97	0.78	0.45	0.59	0.65	2.41
F	1.26	1.06	1.09	1.08	0.38	1.00	1.89	1.21	1.37	0.68
OH	0.33	1.94	1.91	1.97	0.68	1.73	1.15	1.79	1.15	4.00
H_2O					1.32					
ΣCat	12.75	11.83	11.87	11.89	11.66	11.97	11.79	11.84	12.06	23.85

* (1,7) wet chemistry; (2–6, 8–10) electron-microprobe analysis;

** 96.9 wt.% surkhobite + 3.1 wt.% fluorite;

*** Fe^{2+}/Fe^{3+}: (1) wet chemistry; (2) Mössbauer spectroscopy; (3) assigned in accord with (2); (4) Mössbauer spectroscopy; (6) wet chemistry; (7) based on structure refinement results; (8) assigned in accord with (9); (9) Mössbauer spectroscopy.

**** H_2O: (1, 5) TGA; (6, 9) Penfield method; (2, 3, 8) calculated in accord with required number of monovalent anions: OH + F = 3 *pfu* per $(Si_2O_7)_2$; (10) calculated in accord with required number of monovalent anions: OH = 4 *pfu* per $(Si_2O_7)_4$.

Abbreviations: n.r. = not reported; n.a. = not analyzed; n.d. = not detected.

Ref. (1) Hong & Fu (1982); (2) Sokolova *et al.* (2009a); (3) Cámara *et al.* (2016b); (4) Jin *et al.* (2018); (5) Chao (1991); (6) Pekov *et al.* (1999); (7) Eskova *et al.* (2003); (8) taken from IMA No. 06-E and published here for the first time; (9) Rastsvetaeva *et al.* (2008b); (10) Sokolova *et al.* (2015).

high content of Ca and F was due to an admixture of fluorite, which was listed as an associated mineral in Eskova *et al*. (2003). The difference in both Ca and F between the analyses of surkhobite (Table 2 analysis 8) and that given by Eskova *et al*. (2003) (Table 2 analysis 7) corresponds to 3.1 wt.% fluorite. Hence analysis 7 is of a mixture of two minerals: 96.9 wt.% surkhobite and 3.1 wt.% fluorite. For the holotype surkhobite, analysis 8 and analysis 9 of Rastsvetaeva *et al*. (2008b) are in very good agreement, which is not surprising, as they were obtained from the same crystal (see above).

We calculated chemical formulae on the basis of 19 $(O + F)$ *apfu* for analyses 1–9 and 38 $(O + F)$ *apfu* for analysis 10: bobshannonite. In the perraultite-type structure, there are 12 cations *pfu* (24 *pfu* in bobshannonite). The cation sums of 12.75 and 12.06 *apfu* for analyses 1 and 9, respectively, tell us that there are some problems with these two analyses. In a perraultite-type structure with fully occupied cation sites, there is no space for H_2O groups, and hence the presence of 1.32 H_2O *pfu* (analysis 5) is doubtful.

INFRARED SPECTROSCOPY OF JINSHAJIANGITE

Experimental details

Fourier-transform infrared spectra were collected from the single crystal of jinshajiangite from Norra Kärr, Sweden [previously used for X-ray diffraction by Sokolova *et al*. (2009a)]. The lamella, approximately 30 × 40 × 10 μm, was analyzed still mounted on the glass capillary and suspended on the FTIR microscope stage under the IR beam. The data were collected using a Bruker Hyperion 3000 microscope attached to a Vertex V70 optical bench at INFN (Frascati, Italy). A conventional Globar was used as IR source, and the set-up consisted of a KBr beamsplitter and a N2-cooled MCT detector. A total of 128 scans were co-added both on sample and background, for a nominal resolution of 4 cm^{-1}; the beam size was set at ~20 μm^2.

Description of the spectra

The unpolarized FTIR spectra are shown in Figure 1. Two zones with slightly different colors were examined: a brown zone and a yellow zone. The results (Fig. 1a) are almost identical, thus the two zones have no discernable difference. In the principal OH-stretching region (4000–3000 cm^{-1}), the spectra show two sharp peaks at 3630 and 3585 cm^{-1}, with an evident additional band at 3601 cm^{-1} partly overlapping with the 3585 cm^{-1} component; a broader band is also present at 3497 cm^{-1}. In the NIR region, where combination stretching and bending modes are located, a main band is observed at 4220 cm^{-1}, with two minor components at 4142 and 4082 cm^{-1}, respectively. These can be assigned to a combination of stretching plus vibrational modes of the O–H group $(\nu_{OH} + \delta_{OH})$. No absorptions are present at higher wavenumbers (4800–5500 cm^{-1} range) thus excluding the presence of H_2O groups in the jinshajiangite structure.

CRYSTAL STRUCTURE

Experimental details

Here we report structure-refinement results for jinshajiangite from Norra Kärr, Sweden (chemical analysis 2, Table 2) and holotype bobshannonite from Mont Saint-Hilaire, Canada (chemical analysis 10, Table 2). For the holotype surkhobite from the Darai-Pioz massif, Tajikistan (chemical analysis 8, Table 2), we report experimental details of single-crystal X-ray data collection and structure-refinement results. Details of data collection for jinshajiangite from Norra Kärr, Sweden, and bobshannonite can be found in Sokolova *et al*. (2009a) and Sokolova *et al*. (2015); experimental details for single-crystal X-ray data collection for the holotype surkhobite are given below.

Data collection for the holotype surkhobite. In 2016, single-crystal X-ray data for surkhobite were collected using a Bruker APEX II ULTRA three-circle diffractometer equipped with a rotating anode generator (Mo$K\alpha$), multilayer optics, and an APEX II 4K CCD detector. The intensities of reflections were collected with a frame width of 0.3° and a frame time of 2 s. Unit-cell parameters of surkhobite were determined using 7584 reflections $(I > 10\sigma I)$, respectively. An absorption correction was done using the TWINABS program (Sheldrick 2015).

Structure refinement. In this work, we re-integrated previously collected single-crystal X-ray data on two triclinic unit cells: (1) the (Niggli) reduced unit cell, space group $P\bar{1}$, $c \sim 11$ Å, and (2) an unconventional unit cell, space group $C\bar{1}$, $c \sim 11$ Å, to make a comparison with the TS-block structures more straightforward, as the TS-block structures are characterized by two minimal translations, $t_1 \sim 5.4$ and $t_2 \sim 7$ Å. The triclinic $C\bar{1}$ unit cell with $c \sim 21$ Å previously used for jinshajiangite (Table 1, Cámara *et al*. 2016b) and bobshannonite (Table 1, Sokolova *et al*. 2015) and the triclinic $C\bar{1}$ unit cell with $c \sim 11$ Å are related by the transformation matrix ($\bar{1}00$ $0\bar{1}0$ ¼ ¼ ½). An empirical absorption correction for twinned crystals (TWINABS, Sheldrick 2015) was applied. CELL_NOW – Version 2008_2 (Sheldrick 2015) was used to obtain HKLF 5 files. Refinement of the crystal structures of jinshajiangite, surkhobite, and bobshan-

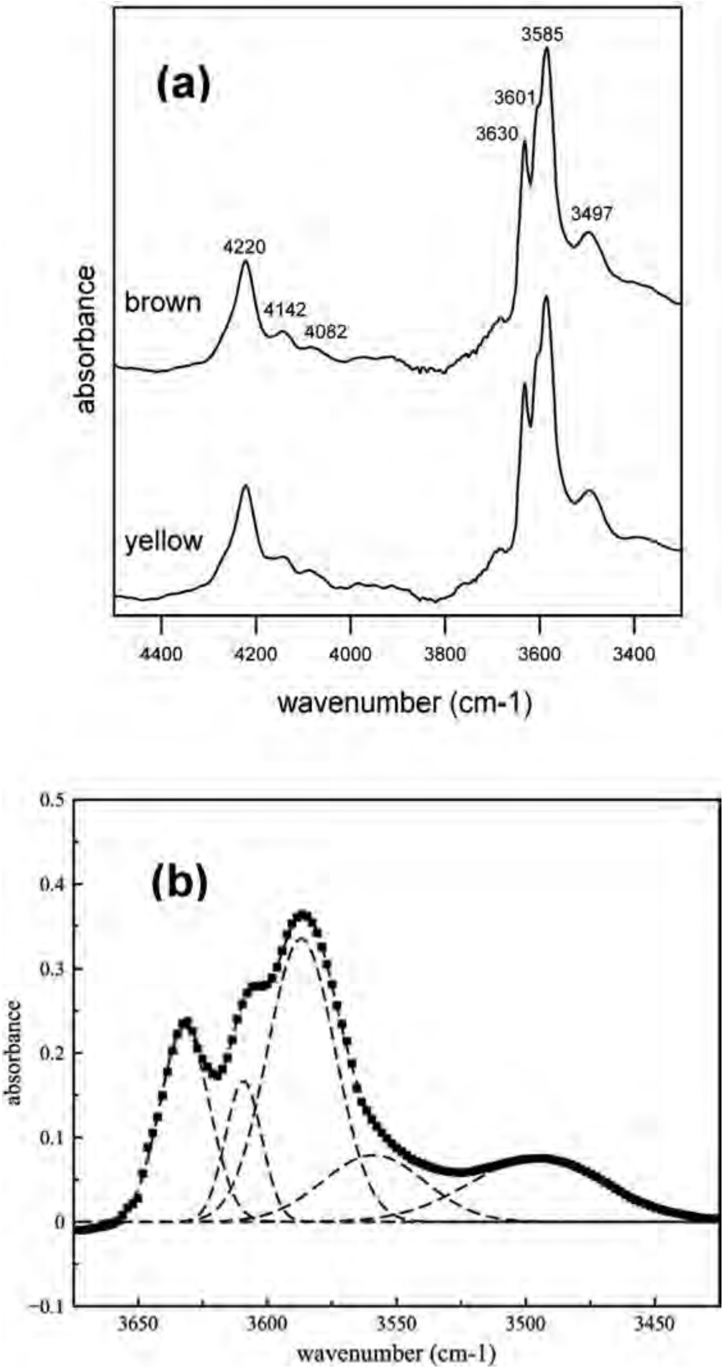

FIG. 1. (a) FTIR spectra of brown and yellow zones of a single crystal of jinshajiangite from Norra Kärr, Sweden; (b) fitted spectrum of the yellow zone in the principal O–H stretching region; heavy dots = observed data, broken lines = component peaks, continuous line: sum of the intensities of the component peaks.

TABLE 3. MISCELLANEOUS STRUCTURE-REFINEMENT DATA* FOR THE PERRAULTITE-TYPE MINERALS

	Jinshajiangite		Surkhobite		Bobshannonite	
Short form of the ideal formula	$NaBaFe^{2+}{}_4Ti_2(Si_2O_7)_2O_2(OH)_2F$		$NaBaMn_4Ti_2(Si_2O_7)_2O_2(OH)_2F$		$Na_2KBa(Mn_7Na)Nb_4(Si_2O_7)_4O_4(OH)_4O_2$	
Space group	$P\bar{1}$	$C\bar{1}$	$P\bar{1}$	$C\bar{1}$	$P\bar{1}$	$C\bar{1}$
a (Å)	8.744(2)	10.720(5)	8.756(5)	10.728(6)	8.812(6)	10.831(7)
b (Å)	8.743(4)	13.823(7)	8.756(5)	13.845(8)	8.813(6)	13.903(9)
c (Å)	11.039(6)	11.044(6)	11.070(6)	11.072(6)	11.149(8)	11.149(8)
α (°)	81.46(1)	108.222(6)	81.458(5)	108.185(6)	81.532(9)	108.145(6)
β (°)	110.26(1)	99.28(1)	110.171(5)	99.219(5)	110.127(7)	99.215(9)
γ (°)	104.44(1)	89.989(6)	104.46(1)	90.001(8)	104.158(6)	90.007(7)
V (Å^3)	765.0(1.1)	1532.0(2.2)	769.7(1.3)	1540.0(2.5)	786.3(1.6)	1572.6(3.2)
Z	2	4	2	4	1	2
Absorption coefficient (mm^{-1})	6.57	6.56	6.60	6.60	6.22	6.22
F(000)	818.2	1636.5	826.5	1653.1	849.7	1699.4
$D_{calc.}$ (g/cm^3)	3.721	3.716	3.750	3.749	3.795	3.796
Crystal description	Golden red prismatic		Brownish-red prismatic		Orange-brown prismatic	
Crystal size (mm)	0.140 × 0.100 × 0.080		0.140 × 0.100 × 0.025		0.012 × 0.010 × 0.003	
Instrument	Bruker AXS SMART APEX		Bruker APEX II ULTRA		Bruker APEX II ULTRA	
$2\theta_{max}$ (°)	60.40	60.40	50.00**	50.00**	61.92	61.96
No. of measured***,	847		7343		7468	
independent and observed	3148	3116	2718	2719	4986	4989
[$F_o > 4\sigma F$] reflections	2813	2746	2651	2657	4945	4963
R_σ (%)	2.97	4.11	1.75	1.99	1.02	1.02
Indices range						
h_{min}, h_{max}	–12, 11	–15, 14	–10, 9	–12, 12	–12, 11	–15, 15
k_{min}, k_{max}	–12, 12	–18, 18	–10, 10	–16, 15	–12, 12	–20, 19
l_{min}, l_{max}	0, 15	0, 15	0, 13	0, 13	0, 16	0, 16
Frame width (°), time (s)	0.2, 30		0.3, 2		0.3, 5	
No. and fraction (%) of	3	3	2	2	2	2
twin domains	53.8(3)	54.8(3)	65.4(2)	65.7(2)	54.7(1)	54.7(1)
	41.5(3)	40.6(3)	34.6(2)	34.3(1)	45.3(1)	45.3(1)
	4.66(6)	4.58(5)				
Final R_{obs} (%)						
$R_1[F_o > 4\sigma F]$, R_1(all)	2.69, 3.44	2.73, 3.53	2.87, 2.90	2.85, 2.88	2.03, 2.04	2.02, 2.03
wR_2	7.17	7.04	8.14	8.01	5.43	5.39
Goodness of fit on F^2	1.075	1.077	1.132	1.024	1.175	1.150
No. refined parameters	312	306	311	311	311	311
$\Delta\rho_{max}$, $\Delta\rho_{min}$ (e^- Å^{-3})	0.93, –0.97	0.75, –0.99	1.32, –1.04	1.34, –1.09	0.89, –1.23	0.91, –1.11

* Crystal system: triclinic; Radiation/monochromator: Mo$K\alpha$/graphite; Absorption correction: TWINABS – Version 2008/2 (Sheldrick 2015); ** Structure refinement; *** HKLF 5.

nonite was done with the Bruker SHELXTL-2014/3 (version 3) system of programs (Sheldrick 2015) in space group $P\bar{1}$ using atom coordinates of Jin *et al.* (2018) and in space group $C\bar{1}$ [both for $P\bar{1}$ and $C\bar{1}$ structure-refinements, coordinates of the H(1) and H(2) atoms were taken from the difference-Fourier map and were included in the refinement]. Scattering curves for neutral atoms were taken from the International Tables for Crystallography (Wilson 1992). To go from the $P\bar{1}$ unit-cell to the $C\bar{1}$ unit cell, we used the following transformation matrix: $(\bar{1}\bar{1}0\ \bar{1}10\ 00\bar{1})$. The final crystal-structure refinements were done on twinned crystals with three twin domains (jinshanjiangite) and two twin domains (surkhobite and bobshannonite). The ratio of twin domains and other miscellaneous information on structure refinement are given in Table 3.

In the perraultite-type structure, there are three groups of cation sites: M^O sites of the O sheet, M^H and *Si* sites of the H sheet, and peripheral A^P and B^P sites which occur in the **I** block; site labelling is in accord with Sokolova (2006). Site-scattering values were refined for the $M^{O}(1–5)$ sites with the scattering curves of Fe (jinshajiangite and surkhobite) and Mn (bobshannonite), $M^{H}(1,2)$ sites with the scattering curves of Ti (jinshajiangite and surkhobite) and Nb (bobshannonite), $A^{P}(1)$ site (Ba), $A^{P}(2)$ site (K), and $B^{P}(1,2)$ sites (Na). The $A^{P}(2)$ site is disordered off the inversion center at ½00, and the two points of the $A^{P}(2)$ site are ~ 1 Å apart. Two H atoms were found in the difference-Fourier map, and the D (donor)–H distances were softly constrained to 0.98 Å. No subsidiary peaks were found in the difference-Fourier map. Tables 4 through 8 contain information pertinent to the structure refinements of jinshajiangite, surkhobite, and bobshannonite in space group $C\bar{1}$: final atom coordinates and equivalent displacement parameters are listed in Table 4, selected distances and angles are given in Table 5, refined site-scattering values and assigned site populations for selected cation and anion sites are given in Table 6, bond-valence values for selected anions in Table 7, and details of hydrogen bonding in Table 8. Crystallography information files (CIF) for jinshajiangite, surkhobite, and bobshannonite for space groups $C\bar{1}$ and $P\bar{1}$ may be obtained from The Depository of Unpublished Data on the MAC website[1].

Site-population assignment

Here we consider the three groups of cation sites: M^{O} sites of the O sheet, M^{H} sites of the H sheet, and peripheral A^{P} and B^{P} sites.

The aggregate refined scattering for the five M^{O} sites is 99.4 *epfu* (jinshajiangite, $Z = 4$), 100.43 *epfu* (surkhobite, $Z = 4$), and 194.0 *epfu* (bobshannonite, $Z = 2$) (Table 6). We assign the following cations which are available from the chemical analyses (Table 2): $Fe^{2+}_{2.83}Mn_{0.63}Fe^{3+}_{0.31}Mg_{0.10}Zr_{0.04}$ *apfu* (jinshajiangite), $Mn_{1.83}Fe^{2+}_{1.77}Fe^{3+}_{0.24}Mg_{0.03}Al_{0.03}$ *apfu* (surkhobite), and $Mn_{6.85}Fe^{2+}_{0.23}Zn_{0.23}Mg_{0.03}Al_{0.02}Zr_{0.04}Na_{0.52}$ *apfu* (bobshannonite), with total calculated scattering values of 100.19, 98.76, and 192.07 *epfu*, respectively (Table 6). The aggregate refined site-scattering values for the five M^{O} sites are in close accord with these compositions. The refined site-scattering values at the five M^{O} sites vary from 24.4 to 25.2 (jinshajiangite), 24.8 to 25.4 (surkhobite), and 23.4 to 25.8 (bobshannonite) electrons per site (normalized per one atom *pfu*). The mean bond-lengths around these sites are very similar (Tables 5, 6), indicating disorder of cations over the five M^{O} sites.

In TS-block minerals, the Ti- and Nb-dominant M^{H} sites are always fully occupied (Sokolova 2006, Sokolova & Cámara 2013). Table 2 gives the available cations: $Ti_{1.99}Nb_{0.01}$ (jinshajiangite, total 2 *apfu*, $Z = 4$), $Ti_{1.82}Nb_{0.10}Zr_{0.08}$ (surkhobite, total 2 *apfu*, $Z = 4$), and $Nb_{2.73}Ti_{1.27}$ (bobshannonite, total 4 *apfu*, $Z = 2$); the aggregate refined scattering at these sites is 44.8 (jinshajiangite), 45.5 (surkhobite), and 141.4 (bobshannonite) *epfu* (Table 6). Hence, in accord with individual refined site-scattering values, we assign Ti + Nb + Zr to the M^{H} sites (Table 6).

There are two A^{P} sites in the crystal structure of perraultite-type minerals. The refined site-scattering values at the $^{[10]}A^{P}(1)$ site (per one atom) and mean bond-lengths $<A^{P}(1)–\varphi>$ (where φ is an unspecified anion) are 52.50 *epfu* and 2.901 Å (jinshajiangite), 54.30 *epfu* and 2.912 Å (surkhobite), and 54.30 *epfu* and 2.922 Å (bobshannonite) (Table 6), and they are consistent with the atomic number and the ionic radius of Ba ($^{[10]}r = 1.52$ Å, Shannon, 1976). Therefore, we assign Ba plus minor vacancy to the $A^{P}(1)$ sites in jinshajiangite and bobshannonite, and Ba plus minor Sr to the $A^{P}(1)$ site in surkhobite (Table 6). The $^{[13]}A^{P}(2)$ site is disordered off the inversion center at ½00, and the two points of the $A^{P}(2)$ site are 1.090, 0.841, and 0.815 Å apart in jinshajiangite, surkhobite, and bobshannonite, respectively (Table 5). Hence in the perraultite-type minerals, the $A^{P}(2)$ site can only be 50% occupied. In jinshajiangite and surkhobite, refined site-scattering values at the $A^{P}(2)$ site are 17.5 and 14.92 *epfu*. The latter values are higher than can be provided by 0.36 K *apfu* and 0.38 K *apfu*, with calculated site-scatterings of 6.84 *epfu* and 7.22 *epfu*, respectively. Therefore, we assign $K_{0.36}Ba_{0.12}$ *apfu* (calculated scattering of 13.56 *epfu*) (jinshajiangite) and $K_{0.38}Ba_{0.10}Cs_{0.02}$ *apfu* (calculated scattering of 13.92 *epfu*) (surkhobite) to the $A^{P}(2)$ site. In accord with the refined site-scattering value of 22.4 *epfu*, we assign $K_{0.93}Rb_{0.07}$ *apfu* to the $A^{P}(2)$ site in bobshannonite (Table 6).

In accord with the refined site-scattering values, we assign Na > Ca (jinshajiangite, surkhobite) and pure Na (bobshannonite) to the $B^{P}(1,2)$ sites (Table 6).

Description of the structure

Topology of the structure. The general topology of the perraultite-type structure is in accord with the recent work on jinshajiangite by Jin *et al*. (2018). In the perraultite-type structure, there is one type of TS (Titanium-Silicate) block and one type of **I** (Intermediate) block; they alternate along **c**. The TS block consists of HOH sheets (H – heteropolyhedral, O – octahedral). The topology of the TS block is as in the bafertisite group of TS-block minerals where Ti (+Nb) = 2 *apfu*: Si_2O_7 groups link to two $(M^{O})^{2+}$ octahedra of

---

[1] http://www.mineralogicalassociation.ca, documents jinshajiangite CM58 19-00070, bobshannonite CM58 19-00070, surkhobite CM58 19-00070.

TABLE 4. ATOM COORDINATES AND ANISOTROPIC DISPLACEMENT PARAMETERS FOR THE PERRAULTITE-TYPE MINERALS, SPACE GROUP $C\bar{1}$

Atom	*x*	*y*	*z*	U_{11}	U_{22}	U_{33}	U_{23}	U_{13}	U_{12}	U_{eq}
					Jinshajiangite					
$M^{O}(1)$	0	0	½	0.0100(17)	0.0086(13)	0.0142(13)	0.0046(10)	0.0037(9)	–0.0026(10)	0.0105(8)
$M^{O}(2)$	½	0	½	0.0048(16)	0.0204(15)	0.0205(13)	0.0140(11)	–0.0012(9)	–0.0038(10)	0.0138(8)
$M^{O}(3)$	0.24857(12)	0.87349(15)	0.48805(9)	0.0089(9)	0.0089(8)	0.0125(5)	0.0054(8)	0.0025(5)	–0.0013(8)	0.0095(4)
$M^{O}(4)$	0.74723(12)	0.87091(15)	0.49059(9)	0.0076(9)	0.0091(8)	0.0120(5)	0.0061(8)	0.0018(5)	–0.0025(8)	0.0089(4)
$M^{O}(5)$	0.49713(15)	0.74658(11)	0.49527(14)	0.0089(10)	0.0082(9)	0.0140(10)	0.0027(8)	–0.0004(6)	–0.0013(7)	0.0108(6)
$M^{H}(1)$	0.53404(16)	0.32140(11)	0.20450(13)	0.0065(10)	0.0055(10)	0.0086(6)	0.0020(5)	0.0017(5)	0.0006(7)	0.0069(5)
$M^{H}(2)$	0.53449(16)	0.78072(12)	0.20332(13)	0.0055(10)	0.0052(10)	0.0092(6)	0.0017(5)	0.0028(5)	0.0007(7)	0.0066(5)
Si(1)	0.7780(3)	0.9503(3)	0.2399(3)	0.0103(17)	0.0061(14)	0.0095(13)	0.0030(11)	0.0037(10)	–0.0044(11)	0.0083(7)
Si(2)	0.3019(3)	0.9512(3)	0.2379(3)	0.0080(17)	0.0061(14)	0.0114(14)	0.0042(11)	0.0011(10)	–0.0026(11)	0.0082(7)
Si(3)	0.7783(3)	0.1691(3)	0.2394(3)	0.0098(17)	0.0070(14)	0.0080(13)	0.0027(10)	0.0015(10)	–0.0044(11)	0.0082(7)
Si(4)	0.3010(3)	0.1695(3)	0.2396(3)	0.0109(17)	0.0068(14)	0.0085(13)	0.0038(11)	0.0037(10)	–0.0018(11)	0.0082(7)
$A^{P}(1)$	0	0	0	0.0124(3)	0.0084(4)	0.01187(19)	0.0039(4)	0.00288(15)	0.0010(5)	0.01065(14)
$A^{P}(2)$	0.4986(4)	0.03963(14)	0.0009(3)	0.0093(7)	0.0354(13)	0.0106(5)	0.0034(14)	0.0018(4)	0.0062(18)	0.0193(4)
$B^{P}(1)$	¼	¼	0	0.031(4)	0.019(3)	0.0062(17)	0.005(3)	0.0041(16)	0.011(3)	0.0185(16)
$B^{P}(2)$	¾	¼	0	0.015(3)	0.016(3)	0.0067(16)	0.005(2)	0.0001(14)	–0.012(2)	0.0124(14)
O(1)	0.9038(7)	0.9194(5)	0.1769(6)	0.018(5)	0.014(4)	0.015(3)	0.012(3)	0.012(3)	0.007(3)	0.0126(16)
O(2)	0.1542(7)	0.9198(5)	0.1765(6)	0.012(4)	0.011(3)	0.016(3)	0.008(3)	–0.000(3)	0.004(3)	0.0123(15)
O(3)	0.6640(7)	0.2206(5)	0.1721(6)	0.010(3)	0.011(2)	0.0142(19)	0.0049(17)	0.005(2)	–0.001(2)	0.0110(11)
O(4)	0.3944(7)	0.2225(5)	0.1741(6)	0.010(3)	0.011(2)	0.0142(19)	0.0049(17)	0.005(2)	–0.001(2)	0.0110(11)
O(5)	0.6623(8)	0.8649(5)	0.1715(7)	0.017(40	0.009(3)	0.016(3)	0.003(2)	0.001(2)	–0.009(3)	0.0145(15)
O(6)	0.3960(8)	0.8656(5)	0.1725(7)	0.021(4)	0.006(3)	0.016(3)	0.001(2)	0.004(3)	–0.000(3)	0.0146(15)
O(7)	0.4027(7)	0.6696(5)	0.1749(6)	0.004(4)	0.013(4)	0.020(3)	0.007(3)	0.003(3)	–0.001(3)	0.0120(15)
O(8)	0.6562(7)	0.6693(5)	0.1725(6)	0.009(4)	0.012(4)	0.015(3)	0.004(3)	0.002(3)	0.007(3)	0.0119(15)
O(9)	0.7237(3)	0.0503(6)	0.2006(3)	0.0137(17)	0.007(2)	0.0157(15)	0.003(3)	0.0019(13)	0.002(4)	0.0123(7)
O(10)	0.3423(3)	0.0504(6)	0.1985(3)	0.0138(17)	0.007(2)	0.0161(15)	0.005(3)	0.0049(13)	0.000(4)	0.0117(7)
O(11)	0.8075(7)	0.9777(7)	0.3958(7)	0.013(5)	0.014(4)	0.008(4)	0.005(3)	0.002(3)	–0.000(3)	0.0109(18)
O(12)	0.3224(7)	0.9805(7)	0.3950(7)	0.009(4)	0.013(4)	0.009(4)	0.005(3)	0.002(3)	–0.002(3)	0.0101(17)
O(13)	0.3104(7)	0.7199(7)	0.3956(7)	0.016(5)	0.010(4)	0.011(4)	0.005(3)	0.002(3)	–0.003(3)	0.0120(19)
O(14)	0.3190(7)	0.2207(7)	0.3965(8)	0.009(5)	0.013(4)	0.014(4)	0.007(3)	0.002(3)	0.000(3)	0.0115(19)
$X^{O}_{M}(1)$	0.5668(5)	0.3563(7)	0.3780(5)	0.009(4)	0.013(4)	0.013(2)	0.004(3)	0.004(2)	–0.001(3)	0.0117(15)
$X^{O}_{M}(2)$	0.5652(6)	0.8334(7)	0.3755(5)	0.015(4)	0.015(4)	0.011(2)	0.006(3)	0.001(2)	–0.004(4)	0.0132(15)
$X^{O}_{A}(1)$	0.5644(6)	0.6020(8)	0.4123(4)	0.019(4)	0.012(3)	0.010(2)	0.004(4)	0.002(2)	–0.002(4)	0.0135(12)
$X^{O}_{A}(2)$	0.5664(5)	0.1055(8)	0.4160(4)	0.008(3)	0.016(3)	0.015(2)	0.009(4)	0.002(2)	–0.000(4)	0.0117(11)
X^{P}_{M}	0.4995(7)	0.2746(2)	0.0004(6)	0.0164(14)	0.0107(19)	0.0105(11)	–0.000(2)	0.0028(10)	–0.006(4)	0.0133(6)
H(1)	0.570(6)	0.587(7)	0.321(2)	0.01625(0)*						
H(2)	0.554(7)	0.104(5)	0.326(2)	0.01405(0)*						

TABLE 4. CONTINUED.

Atom	*x*	*y*	*z*	U_{11}	U_{22}	U_{33}	U_{23}	U_{13}	U_{12}	U_{eq}
					Surkhobite					
M^{O}(1)	0	0	½	0.0065(6)	0.0048(6)	0.0134(6)	–0.0004(5)	0.0022(4)	–0.0003(5)	0.0089(4)
M^{O}(2)	½	0	½	0.0078(7)	0.0206(7)	0.0243(7)	0.0130(6)	–0.0031(5)	–0.0058(6)	0.0168(5)
M^{O}(3)	0.24842(5)	0.87355(7)	0.48793(5)	0.0070(3)	0.0069(4)	0.0115(4)	0.0000(4)	0.0021(2)	–0.0001(4)	0.0090(3)
M^{O}(4)	0.74684(5)	0.87102(7)	0.49046(5)	0.0074(4)	0.0069(4)	0.0118(4)	0.0003(4)	0.0024(2)	–0.0007(4)	0.0092(3)
M^{O}(5)	0.49763(5)	0.74737(5)	0.49554(6)	0.0071(6)	0.0084(5)	0.0152(6)	–0.0021(4)	0	0.0005(4)	0.0118(4)
M^{H}(1)	0.53402(6)	0.32019(5)	0.20290(6)	0.0031(4)	0.0049(5)	0.0079(4)	0.0023(3)	0.0021(3)	0.0010(3)	0.0051(3)
M^{H}(2)	0.53375(6)	0.78106(5)	0.20109(6)	0.0031(4)	0.0036(5)	0.0085(4)	0.0022(3)	0.0021(3)	0.0007(3)	0.0049(3)
Si(1)	0.77802(13)	0.95029(10)	0.23948(13)	0.0064(6)	0.0049(7)	0.0087(7)	–0.0002(5)	0.0025(5)	–0.0004(5)	0.0071(3)
Si(2)	0.30154(13)	0.95130(10)	0.23798(13)	0.0062(6)	0.0045(6)	0.0089(7)	–0.0002(5)	0.0022(5)	–0.0001(5)	0.0070(3)
Si(3)	0.77838(13)	0.16851(10)	0.23875(13)	0.0060(6)	0.0057(7)	0.0077(7)	–0.0004(5)	0.0018(5)	–0.0003(5)	0.0070(3)
Si(4)	0.30045(13)	0.16922(10)	0.23837(13)	0.0061(6)	0.0052(7)	0.0078(7)	–0.0002(5)	0.0016(5)	–0.0010(5)	0.0069(3)
A^{P}(1)	0	0	0	0.0102(2)	0.0088(2)	0.0089(2)	0.0005(2)	0.00221(12)	0.0002(2)	0.0097(14)
A^{P}(2)	0.4982(3)	0.0291(2)	–0.0044(3)	0.0164(7)	0.0808(18)	0.0219(8)	0.0269(13)	0.0050(5)	0.0066(13)	0.0370(6)
B^{P}(1)	¼	¼	0	0.0173(10)	0.0126(10)	0.0046(8)	–0.0007(10)	0.0022(6)	0.0104(11)	0.0123(6)
B^{P}(2)	¾	¼	0	0.0129(9)	0.0104(10)	0.0036(8)	–0.0013(10)	0.0017(6)	–0.0080(10)	0.0098(6)
O(1)	0.9031(3)	0.9187(3)	0.1759(3)	0.0109(15)	0.0129(16)	0.0149(16)	0.0069(14)	0.0036(12)	0.0028(13)	0.0121(7)
O(2)	0.1561(3)	0.9175(3)	0.1737(3)	0.0086(15)	0.0135(16)	0.0143(15)	0.0081(13)	–0.0000(12)	–0.0023(13)	0.0115(7)
O(3)	0.6640(3)	0.2209(2)	0.1732(3)	0.0122(16)	0.0091(15)	0.0125(15)	0.0039(13)	0.0043(12)	0.0022(13)	0.0109(7)
O(4)	0.3939(3)	0.2218(2)	0.1742(3)	0.0098(15)	0.0109(15)	0.0127(15)	0.0051(13)	0.0037(12)	0.0001(12)	0.0106(6)
O(5)	0.6640(3)	0.8650(3)	0.1712(3)	0.0093(15)	0.0108(16)	0.0123(15)	0.0025(13)	0.0024(12)	–0.0014(13)	0.0110(7)
O(6)	0.3942(3)	0.8658(2)	0.1725(3)	0.0087(15)	0.0080(15)	0.0138(15)	0.0029(13)	0.0015(12)	0.0031(12)	0.0104(7)
O(7)	0.4021(3)	0.6698(3)	0.1738(3)	0.0104(15)	0.0108(16)	0.0160(16)	0.0045(13)	0.0068(12)	–0.0001(13)	0.0118(7)
O(8)	0.6550(3)	0.6697(3)	0.1723(3)	0.0097(15)	0.0114(16)	0.0170(16)	0.0039(14)	0.0017(12)	0.0009(13)	0.0129(7)
O(9)	0.7256(2)	0.0500(3)	0.2022(2)	0.0100(12)	0.0092(14)	0.0137(13)	0.0034(14)	0.0006(10)	0.0014(13)	0.0112(6)
O(10)	0.3407(2)	0.0504(3)	0.1989(2)	0.0131(13)	0.0079(13)	0.0131(13)	0.0032(13)	0.0055(10)	0.0016(13)	0.0110(5)
O(11)	0.8073(3)	0.9769(3)	0.3952(3)	0.0088(17)	0.0087(17)	0.0113(18)	0.0002(15)	0.0036(14)	–0.0003(15)	0.0101(8)
O(12)	0.3209(3)	0.9801(3)	0.3940(4)	0.0098(18)	0.0089(18)	0.0119(18)	0.0001(15)	0.0036(14)	–0.0004(15)	0.0107(8)
O(13)	0.3102(3)	0.7191(3)	0.3945(3)	0.0085(17)	0.0092(18)	0.0081(17)	–0.0022(15)	0.0020(14)	–0.0013(15)	0.0097(8)
O(14)	0.3186(3)	0.2198(3)	0.3939(3)	0.0081(17)	0.0075(17)	0.0081(17)	–0.0018(15)	0.0019(13)	–0.0000(14)	0.0088(7)
X$^{O}_{M}$(1)	0.5657(3)	0.3553(3)	0.3764(3)	0.0098(13)	0.0100(18)	0.0120(13)	0.0013(14)	0.0032(10)	0.0006(14)	0.0109(7)
X$^{O}_{M}$(2)	0.5643(3)	0.8323(3)	0.3738(3)	0.0101(13)	0.015(2)	0.0118(13)	0.0035(14)	0.0022(10)	–0.0008(14)	0.0124(7)
X$^{O}_{A}$(1)	0.5646(2)	0.6019(4)	0.4108(3)	0.0112(13)	0.0115(16)	0.0120(13)	0.0027(19)	0.0035(10)	0.0010(19)	0.0116(6)
X$^{O}_{A}$(2)	0.5647(2)	0.1048(4)	0.4147(3)	0.0115(13)	0.0132(17)	0.0119(13)	0.0029(19)	0.0022(10)	0.0011(18)	0.0124(6)
X$^{P}_{M}$	0.5006(3)	0.27322(16)	0.0010(2)	0.0158(11)	0.0163(12)	0.0085(11)	0.0022(11)	0.0019(8)	0.0007(11)	0.0139(5)
H(1)	0.558(4)	0.598(4)	0.3207(17)	0.01393(0)*						
H(2)	0.556(4)	0.100(4)	0.3236(16)	0.01492(0)*						

TABLE 4. CONTINUED.

Atom	*x*	*y*	*z*	U_{11}	U_{22}	U_{33}	U_{23}	U_{13}	U_{12}	U_{eq}
					Bobshannonite					
$M^{O}(1)$	0	0	½	0.0070(3)	0.0106(3)	0.0135(3)	0.0039(2)	0.0009(2)	0.0004(2)	0.01040(18)
$M^{O}(2)$	½	0	½	0.0101(4)	0.0458(5)	0.0396(5)	0.0343(4)	–0.0100(3)	–0.0108(4)	0.0286(3)
$M^{O}(3)$	0.24821(2)	0.87328(5)	0.48720(3)	0.00796(14)	0.00940(19)	0.01074(14)	0.0030(2)	0.00166(9)	0.0002(3)	0.00939(9)
$M^{O}(4)$	0.74673(3)	0.87076(5)	0.48958(3)	0.00842(14)	0.01019(19)	0.01128(14)	0.0038(2)	0.00151(9)	–0.0007(3)	0.00988(10)
$M^{O}(5)$	0.49840(3)	0.74829(3)	0.49384(4)	0.0085(3)	0.0092(3)	0.0226(3)	–0.0016(2)	–0.0027(2)	0.0017(3)	0.01557(19)
$M^{H}(1)$	0.53191(2)	0.31695(2)	0.19239(2)	0.00582(9)	0.00734(12)	0.01225(10)	0.00375(7)	0.00215(6)	0.00071(6)	0.00824(7)
$M^{H}(2)$	0.53159(2)	0.77910(2)	0.18987(2)	0.00580(9)	0.00756(12)	0.01350(10)	0.00363(7)	0.00224(6)	0.00063(6)	0.00881(7)
Si(1)	0.77916(8)	0.95100(6)	0.23907(7)	0.0065(3)	0.0054(3)	0.0058(3)	0.0016(2)	0.0005(2)	–0.0005(2)	0.00598(14)
Si(2)	0.30009(7)	0.95155(6)	0.23744(7)	0.0054(3)	0.0056(3)	0.0059(3)	0.0018(2)	0.0018(2)	0.0013(2)	0.00553(14)
Si(3)	0.77861(8)	0.16768(6)	0.23995(8)	0.0063(3)	0.0079(3)	0.0082(3)	0.0026(2)	0.0025(2)	0.0001(2)	0.00730(14)
Si(4)	0.29986(8)	0.16795(6)	0.23913(8)	0.0074(3)	0.0080(3)	0.0086(3)	0.0026(2)	0.0007(2)	0.0006(2)	0.00807(16)
$A^{P}(1)$	0	0	0	0.01236(8)	0.01241(10)	0.01125(8)	0.00233(11)	0.00180(5)	0.00018(11)	0.01236(5)
$A^{P}(2)$	0.4986(3)	0.02860(15)	–0.0026(3)	0.0216(4)	0.0782(13)	0.0249(5)	0.0168(10)	0.0048(3)	0.0042(11)	0.0414(4)
$B^{P}(1)$	¼	¼	0	0.0351(8)	0.0253(9)	0.0110(6)	0.0004(10)	0.0021(5)	0.0157(11)	0.0253(5)
$B^{P}(2)$	¾	¼	0	0.0344(8)	0.0250(9)	0.0108(6)	0.0005(10)	0.0025(5)	–0.0147(11)	0.0248(5)
O(1)	0.90416(14)	0.92026(13)	0.17748(15)	0.0095(6)	0.0111(7)	0.0136(7)	0.0056(5)	0.0057(5)	0.0039(5)	0.0106(3)
O(2)	0.15481(14)	0.91909(13)	0.17446(15)	0.0075(6)	0.0122(7)	0.0126(6)	0.0055(6)	0.0001(5)	–0.0004(5)	0.0106(3)
O(3)	0.66596(14)	0.22081(12)	0.17398(14)	0.0105(6)	0.0115(7)	0.0121(6)	0.0051(6)	0.0021(5)	0.0036(5)	0.0110(3)
O(4)	0.39275(14)	0.22117(12)	0.17452(14)	0.0104(6)	0.0114(7)	0.0118(6)	0.0050(5)	0.0017(5)	–0.0026(5)	0.0109(3)
O(5)	0.66575(14)	0.86603(12)	0.17218(14)	0.0106(6)	0.0090(7)	0.0113(6)	0.0014(5)	0.0015(5)	–0.0030(5)	0.0107(3)
O(6)	0.39236(14)	0.86681(12)	0.17330(14)	0.0104(6)	0.0085(7)	0.0127(6)	0.0016(5)	0.0032(5)	0.0036(5)	0.0108(3)
O(7)	0.40340(14)	0.66866(13)	0.17602(14)	0.0091(6)	0.0111(7)	0.0122(6)	0.0020(5)	0.0044(5)	–0.0001(5)	0.0109(3)
O(8)	0.65522(14)	0.66834(12)	0.17335(15)	0.0080(6)	0.0099(7)	0.0130(6)	0.0022(5)	0.0005(5)	0.0022(5)	0.0108(3)
O(9)	0.72652(11)	0.05009(13)	0.20018(12)	0.0098(5)	0.0073(6)	0.0140(5)	0.0041(6)	0.0003(4)	0.0001(6)	0.0104(2)
O(10)	0.3388(11)	0.05011(13)	0.19760(12)	0.0114(5)	0.0077(6)	0.0148(5)	0.0049(6)	0.0046(4)	0.0007(6)	0.0107(2)
O(11)	0.8092(2)	0.9780(2)	0.3934(2)	0.0127(10)	0.0197(10)	0.0064(8)	0.0036(8)	0.0011(7)	0.0004(8)	0.0131(4)
O(12)	0.3211(2)	0.9798(2)	0.3918(2)	0.0086(8)	0.0194(10)	0.0064(7)	0.0042(7)	0.0009(7)	–0.0021(7)	0.0115(4)
O(13)	0.3088(2)	0.7195(2)	0.3932(2)	0.0075(9)	0.0101(8)	0.0092(8)	0.0033(7)	0.0018(7)	0.0007(7)	0.0088(4)
O(14)	0.3173(2)	0.2198(2)	0.3925(2)	0.0095(8)	0.0097(8)	0.0092(8)	0.0032(7)	0.0013(7)	–0.0005(7)	0.0094(4)
$X^{O}_{M}(1)$	0.56423(13)	0.35480(18)	0.37131(13)	0.0114(6)	0.0136(10)	0.0083(5)	0.0014(6)	0.0010(4)	0.0014(6)	0.0117(4)
$X^{O}_{M}(2)$	0.56377(13)	0.83081(19)	0.36904(13)	0.0114(6)	0.0179(12)	0.0092(5)	0.0028(6)	0.0011(4)	–0.0006(6)	0.0132(4)
$X^{O}_{A}(1)$	0.56315(13)	0.6015(2)	0.41079(12)	0.0149(6)	0.0128(8)	0.0098(5)	0.0040(11)	0.0019(4)	0.0072(12)	0.0125(2)
$X^{O}_{A}(2)$	0.56331(12)	0.1034(2)	0.41355(12)	0.0115(5)	0.0150(9)	0.0117(5)	0.0051(11)	0.0013(4)	0.0067(11)	0.0126(2)
X^{P}_{M}	0.50053(15)	0.27383(9)	0.00086(14)	0.0099(5)	0.0119(6)	0.0052(5)	0.0015(5)	0.0010(4)	0.0001(5)	0.0093(2)
H(1)	0.546(3)	0.595(2)	0.3209(12)	0.01494(0)*						
H(2)	0.541(3)	0.103(2)	0.3250(13)	0.01512(0)*						

* U_{iso}

the O sheet adjacent along $\mathbf{t_2}$. In the O sheet, there are five $^{[6]}M^{O}$ sites occupied mainly by divalent cations Fe^{2+} and Mn. In the H sheet, two $^{[6]}M^{H}$ sites are occupied mainly by Ti (+ Nb). The M^{H} octahedra and Si_2O_7 groups constitute the H sheet. The TS blocks link *via* common vertices of M^{H} octahedra, *i.e.*, M^{H}–X^{P}_{M}–M^{H} bridges. In the **I** block, there are $A^{P}(1)$ and $A^{P}(2)$ sites, occupied mainly by Ba and K, respectively, and two Na-dominant $B^{P}(1,2)$ sites.

Sokolova & Cámara (2016) described two rings of polyhedra in the H sheet of TS-block minerals with double t_1 and t_2 translations: (1) the six-membered A^{P} ring consists of six polyhedra: four SiO_4 tetrahedra (two Si_2O_7 groups) and two M^{H} octahedra, and (2) the four-membered B^{P} ring consists of four polyhedra: two SiO_4 tetrahedra and two M^{H} octahedra. In perraultite-type minerals, the six-membered $A^{P}(1)$ ring is shortened along $\mathbf{t_2}$ and the six-membered $A^{P}(2)$ ring is elongated along $\mathbf{t_2}$ (*cf.* jinshajiangite, Fig. 2c–f). Sokolova & Cámara (2016) showed that this distortion of rings of polyhedra is necessary to satisfy bond-valence requirements at the X^{P}_{M} anions, where X^{P}_{M} = F, O. Distortion of the H-sheet polyhedra in jinshajiangite was described by Cámara *et al.* (2016b).

Cation and anion sites. The cation sites are divided into three groups: M^{O} sites of the O sheet, M^{H} and *Si* sites of the H sheet, and peripheral A^{P} and B^{P} sites which occur in the **I** block. In accord with Sokolova (2006), we label the X anions as follows: X^{O}_{M} = a common anion for three M^{O} and one M^{H} cations; X^{O}_{A} = a common anion for three M^{O} cations located approximately under the A^{P} site; X^{P}_{M} = an apical anion of an M^{H} cation at the periphery of the TS block (a bridge anion between two M^{H} cations) (Fig. 2a–c).

In the O sheet of jinshajiangite (and surkhobite plus bobshannonite), there are five Fe^{2+}-dominant and five Mn-dominant M^{O} sites, respectively (Table 6). The $M^{O}(1,2,5)$ atoms are coordinated by four O atoms and two monovalent X^{O}_{A} anions, with $\langle M^{O}-\varphi\rangle = 2.166$–$2.298$ Å. The $M^{O}(3,4)$ atoms are coordinated by five O atoms and a monovalent X^{O}_{A} anion, with $\langle M^{O}-\varphi\rangle =$ 2.176–2.226 Å (Tables 5, 6). There is no discernible order of Fe^{2+} and Mn at the $M^{O}(1$–$5)$ sites in the O sheets of jinshajiangite, surkhobite, and bobshannonite. In jinshajiangite and surkhobite, Fe^{2+}-dominant and Mn-dominant M^{O} sites give ideally Fe^{2+}_{4} and Mn_4 *apfu* ($Z = 4$) (Table 6). In bobshannonite, the O sheet has the following composition: $[(Mn_{6.85}Fe_{0.23}Zn_{0.23}Mg_{0.03})^{2+}_{\Sigma 7.34}Na^{+}_{0.52}Al^{3+}_{0.02}Zr^{4+}_{0.04}\square_{0.12}]$ *pfu* ($Z = 2$), with a total charge of 15.42^{+}. Note that the O sheet has a significant amount of monovalent Na (shown in bold). We write the ideal composition of the O sheet as (Mn_7Na) *apfu*, with a corresponding charge of 15+.

In the H sheets, two Ti-dominant (jinshajiangite, surkhobite) and Nb-dominant (bobshannonite) M^{H} sites are coordinated by five O atoms and an X^{P}_{M} anion (Fig. 2a, c), with $\langle M^{H}-\varphi\rangle$ = 1.967, 1.968 Å (jinshajiangite, surkhobite) and 1.973 Å (bobshannonite) (Tables 5, 6). The four tetrahedrally coordinated *Si* sites are occupied by Si, with $\langle Si-O\rangle$ = 1.624 Å (Table 5). The M^{H} sites of the two H sheets give ideally Ti_2 *apfu* (jinshajiangite, surkhobite, $Z = 4$) and Nb_4 *apfu* (bobshannonite, $Z = 2$).

The peripheral A^{P} and B^{P} sites are shifted from the H sheets of the TS block and occur in the **I** block (Fig. 2a, c–f). The $A^{P}(1)$ site is occupied by Ba at 92% in jinshajiangite and at 95% in bobshannonite (Table 6). In surkhobite, the $A^{P}(1)$ site is fully occupied by Ba plus minor Sr (Table 6). The $A^{P}(1)$ site is coordinated by eight O atoms and two F atoms (X^{P}_{M} site) in jinshajiangite and surkhobite, with $\langle A^{P}(1)-\varphi\rangle$ = 2.901 and 2.912 Å [Figure 2d shows the $A^{P}(1)$ cage; Tables 5, 6]. In bobshannonite, the $A^{P}(1)$ site is coordinated by eight O atoms and two X^{P}_{M} anions (O and F), with $\langle A^{P}(1)-\varphi\rangle = 2.922$ Å (Tables 5, 6). As mentioned above, the $^{[13]}A^{P}(2)$ site is disordered off the inversion center at ½00, and the two points of the $A^{P}(2)$ site are 1.090, 0.841, and 0.815 Å apart in jinshajiangite (Fig. 2a, c, f), surkhobite, and bobshannonite, respectively (Table 5). The topology of the $A^{P}(2)$ cage is identical in jinshajiangite, surkhobite, and bobshannonite (Fig. 2f). In the perraultite-type minerals, the $A^{P}(2)$ site is ≤50% occupied: in jinshajiangite and surkhobite by $K_{0.36}Ba_{0.12}\square_{0.52}$ *pfu* and $K_{0.38}Ba_{0.10}Cs_{0.02}\square_{0.50}$ *pfu* ($Z = 4$), in bobshannonite by $K_{0.93}Rb_{0.07}\square_{1.00}$ *pfu* ($Z = 2$) (Table 6). The $A^{P}(2)$ site is coordinated by 12 O atoms and one F atom (X^{P}_{M} site) in jinshajiangite and surkhobite, with $\langle A^{P}(2)-\varphi\rangle$ = 3.240 and 3.251 Å (Fig. 2f; Tables 5, 6). In bobshannonite, the $A^{P}(2)$ site is coordinated by 12 O atoms and one X^{P}_{M} anion. Where the X^{P}_{M} site is coordinated by two Nb atoms at the M^{H} site, the X^{P}_{M} site is occupied by an O atom. Where the X^{P}_{M} site is coordinated by two Ti atoms or one Nb atom plus one Ti atom at the M^{H} site, the X^{P}_{M} site is occupied by a F atom, $\langle A^{P}(2)-\varphi\rangle = 3.276$ Å (Tables 5, 6). Inspection of Table 5 shows that for jinshajiangite there are nine short bonds $A^{P}(2)-\varphi$ = 2.927–3.250 Å and four long bonds $A^{P}(2)-\varphi$ = 3.758–3.810 Å [Figure 2f shows the $A^{P}(2)$ cage in with the four long bonds to the right of the central $A^{P}(2)$ atom]. The four long bonds are necessary to make the coordination sphere of the $A^{P}(2)$ atom complete. Jin *et al.* (2018) erroneously reported [9]-coordination of the $A^{P}(2)$ site in jinshajangite. In jinshajiangite and surkhobite, the aggregate content of the two A^{P} sites is $Ba_{0.58}K_{0.36}\square_{0.06}$ *pfu* and $Ba_{0.59}K_{0.38}Cs_{0.02}Sr_{0.01}$ *apfu*, respectively, ideally Ba *apfu* ($Z = 4$). In bobshannonite, Ba:K ~ 1:1 (Table 2, analysis 10), hence the contents of Ba and K are lower and higher, respectively, when compared to jinshajian-

TABLE 5. SELECTED INTERATOMIC DISTANCES (Å) AND ANGLES (°) IN THE PERRAULTITE-TYPE MINERALS, SPACE GROUP $C\overline{1}$

	Jinshajiangite		Surkhobite		Bobshannonite	
M^{O}(1)–X$^{O}_{A}$(1)a	2.115(9)	×2	2.130(5)	×2	2.131(3)	×2
M^{O}(1)–O(11)b	2.166(8)	×2	2.173(4)	×2	2.183(3)	×2
M^{O}(1)–X$^{O}_{M}$(1)a	2.216(8)	×2	2.232(4)	×2	2.266(2)	×2
<M^{O}(1)–φ>	2.166		2.178		2.193	
M^{O}(2)–O(12)b	2.034(8)	×2	2.055(4)	×2	2.081(3)	×2
M^{O}(2)–X$^{O}_{A}$(2)	2.131(9)	×2	2.132(5)	×2	2.130(3)	×2
M^{O}(2)–X$^{O}_{M}$(2)b	2.452(8)	×2	2.470(4)	×2	2.515(3)	×2
<M^{O}(2)–φ>	2.207		2.219		2.242	
M^{O}(3)–X$^{O}_{A}$(2)b	2.067(6)		2.092(3)		2.133(2)	
M^{O}(3)–X$^{O}_{M}$(1)k	2.094(6)		2.112(3)		2.162(2)	
M^{O}(3)–O(11)c	2.200(9)		2.212(4)		2.233(3)	
M^{O}(3)–O(13)	2.203(9)		2.218(4)		2.271(3)	
M^{O}(3)–O(13)l	2.239(8)		2.244(4)		2.130(3)	
M^{O}(3)–O(12)	2.254(8)		2.253(5)		2.280(3)	
<M^{O}(3)–φ>	2.176		2.188		2.202	
M^{O}(4)–X$^{O}_{A}$(1)d	2.102(6)		2.113(3)		2.150(2)	
M^{O}(4)–X$^{O}_{M}$(2)	2.117(6)		2.133(3)		2.174(2)	
M^{O}(4)–O(14)e	2.211(9)		2.232(4)		2.238(3)	
M^{O}(4)–O(11)	2.209(8)		2.205(5)		2.250(3)	
M^{O}(4)–O(14)b	2.222(8)		2.238(4)		2.263(3)	
M^{O}(4)–O(12)c	2.248(9)		2.251(4)		2.282(3)	
<M^{O}(4)–φ>	2.185		2.195		2.226	
M^{O}(5)–O(13)	2.096(8)		2.111(4)		2.149(3)	
M^{O}(5)–X$^{O}_{A}$(1)	2.10(1)		2.119(5)		2.132(3)	
M^{O}(5)–O(14)b	2.103(8)		2.115(4)		2.151(3)	
M^{O}(5)–X$^{O}_{A}$(2)b	2.14(1)		2.138(5)		2.159(3)	
M^{O}(5)–X$^{O}_{M}$(2)	2.242(8)		2.239(4)		2.250(2)	
M^{O}(5)–X$^{O}_{M}$(1)b	2.451(8)		2.462(4)		2.538(2)	
<M^{O}(5)–φ>	2.189		2.197		2.298	
M^{H}(1)–X$^{O}_{M}$(1)	1.798(5)		1.803(3)		1.871(2)	
M^{H}(1)–O(4)	1.943(7)		1.947(3)		1.955(2)	
M^{H}(1)–O(3)	1.965(7)		1.951(3)		1.965(2)	
M^{H}(1)–O(2)f	1.999(8)		2.010(3)		2.022(2)	
M^{H}(1)–O(1)a	1.999(7)		2.010(3)		2.020(2)	
M^{H}(1)–X$^{P}_{M}$	2.111(6)		2.094(3)		2.001(2)	
<M^{H}(1)–φ>	1.969		1.969		1.972	
M^{H}(2)–X$^{O}_{M}$(2)	1.786(5)		1.794(3)		1.874(2)	
M^{H}(2)–O(5)	1.940(7)		1.949(3)		1.962(2)	
M^{H}(2)–O(6)	1.945(8)		1.948(3)		1.961(2)	
M^{H}(2)–O(8)	2.001(7)		1.999(3)		2.025(2)	
M^{H}(2)–O(7)	2.003(7)		2.007(3)		2.023(2)	
M^{H}(2)–(X$^{P}_{M}$)g	2.107(6)		2.096(3)		1.993(2)	
<M^{H}(2)–φ>	1.964		1.966		1.973	
Si(1)–O(1)	1.613(8)		1.612(3)		1.613(2)	
Si(1)–O(11)	1.620(8)		1.624(4)		1.620(3)	
Si(1)–O(5)	1.626(8)		1.615(3)		1.618(2)	
Si(1)–O(9)h	1.654(9)		1.635(4)		1.644(2)	
<Si(1)–O>	1.628		1.622		1.624	
Si(2)–O(2)	1.620(8)		1.611(3)		1.619(2)	
Si(2)–O(6)	1.625(8)		1.616(3)		1.613(2)	
Si(2)–O(12)	1.632(8)		1.625(4)		1.619(3)	
Si(2)–O(10)h	1.640(8)		1.635(4)		1.640(2)	
<Si(2)–O>	1.629		1.622		1.623	

TABLE 5. CONTINUED.

	Jinshajiangite		Surkhobite		Bobshannonite	
Si(3)–O(3)	1.611(8)		1.613(3)		1.621(2)	
Si(3)–O(7)f	1.611(8)		1.611(3)		1.628(2)	
Si(3)–O(13)f	1.625(8)		1.625(4)		1.612(3)	
Si(3)–O(9)	1.644(9)		1.640(4)		1.630(2)	
<Si(3)–O>	1.623		1.622		1.623	
Si(4)–O(8)a	1.608(8)		1.615(3)		1.621(2)	
Si(4)–O(4)	1.620(7)		1.610(3)		1.626(2)	
Si(4)–O(14)	1.633(8)		1.623(4)		1.615(3)	
Si(4)–O(10)	1.646(8)		1.643(4)		1.633(2)	
<Si(4)–O>	1.627		1.623		1.624	
Si(1)i–O(9)–Si(3)	133.2(2)		134.8(2)		133.61(9)	
Si(2)i–O(10)–Si(4)	132.8(2)		133.9(2)		133.17(9)	
<Si–O–Si>	133.0		134.4		133.39	
A^{P}(1)–O(8)a	2.845(7)	×2	2.848(3)	×2	2.860(2)	×2
A^{P}(1)–O(2)i	2.842(7)	×2	2.854(3)	×2	2.860(2)	×2
A^{P}(1)–O(7)a	2.851(7)	×2	2.856(3)	×2	2.870(2)	×2
A^{P}(1)–O(1)g	2.852(6)	×2	2.857(3)	×2	2.872(2)	×2
A^{P}(1)–(X$^{P}_{M}$)a	3.117(3)	×2	3.143(3)	×2	3.148(2)	×2
<A^{P}(1)–φ>	2.901		2.912		2.922	
A^{P}(2)–O(10)	2.927(5)		2.969(4)		2.982(3)	
A^{P}(2)–O(9)j	2.955(5)		2.929(4)		2.962(3)	
A^{P}(2)–O(9)	2.965(5)		3.011(4)		3.014(3)	
A^{P}(2)–O(10)j	2.967(5)		2.923(4)		2.963(3)	
A^{P}(2)–O(5)g	2.975(8)		3.042(4)		3.088(3)	
A^{P}(2)–O(6)g	2.988(7)		3.048(4)		3.095(3)	
A^{P}(2)–O(3)	2.990(7)		3.115(5)		3.144(3)	
A^{P}(2)–O(4)	2.994(7)		3.115(4)		3.133(3)	
A^{P}(2)–X$^{P}_{M}$	3.250(3)		3.362(3)		3.398(3)	
A^{P}(2)–O(6)i	3.758(7)		3.695(4)		3.701(3)	
A^{P}(2)–O(5)i	3.775(8)		3.709(4)		3.714(3)	
A^{P}(2)–O(3)j	3.776(7)		3.664(5)		3.692(4)	
A^{P}(2)–O(4)j	3.810(7)		3.683(5)		3.701(3)	
<A^{P}(2)–φ>	3.240		3.251		3.276	
A^{P}(2)–A^{P}(2)j	1.090(3)		0.841(4)		0.815(3)	
B^{P}(1)–O(5)a	2.385(7)	×2	2.378(3)	×2	2.399(2)	×2
B^{P}(1)–O(4)	2.394(7)	×2	2.402(3)	×2	2.421(2)	×2
B^{P}(1–X$^{P}_{M}$	2.695(7)	×2	2.706(3)	×2	2.732(2)	×2
B^{P}(1)–O(8)a	2.798(7)	×2	2.804(4)	×2	2.843(2)	×2
B^{P}(1)–O(1)a	2.849(8)	×2	2.843(3)	×2	2.886(2)	×2
<B^{P}(1)–φ>	2.624		2.627		2.656	
B^{P}(2)–O(3)	2.382(6)	×2	2.396(3)	×2	2.411(2)	×2
B^{P}(2)–O(6)g	2.402(7)	×2	2.399(3)	×2	2.416(2)	×2
B^{P}(2)–X$^{P}_{M}$	2.708(7)	×2	2.696(3)	×2	2.724(2)	×2
B^{P}(2)–O(7)g	2.823(7)	×2	2.815(4)	×2	2.869(2)	×2
B^{P}(2)–O(2)g	2.854(7)	×2	2.815(3)	×2	2.858(2)	×2
<B^{P}(2)–φ>	2.633		2.624		2.656	

φ – unspecified anion: O, OH, F. Symmetry operators: a: $x - {}^1/_2$, $y - {}^1/_2$, z; b: $-x + 1$, $-y + 1$, $-z + 1$; c: $-x + 1$, $-y + 2$, $-z + 1$; d: $-x + {}^3/_2$, $-y + {}^1/_2$, $-z + 1$; e: $x + {}^1/_2$, $y + {}^1/_2$, z; f: $x + {}^1/_2$, $y - {}^1/_2$, z; g: $-x + 1$, $-y + 1$, $-z$; h: x, $y + 1$, z; i: x, $y - 1$, z; j: $-x + 1$, $-y$, $-z$; k: $x - {}^1/_2$, $y + {}^1/_2$, z; l: $-x + {}^1/_2$, $-y + {}^3/_2$, $-z + 1$.

TABLE 6. REFINED SITE-SCATTERING AND ASSIGNED SITE-POPULATIONS FOR THE PERRAULTITE-TYPE MINERALS, SPACE GROUP $C\bar{1}$

Site*	Refined site-scattering (*epfu*)	Assigned site-population (*pfu*)	Calculated site-scattering (*epfu*)	$\langle \mathrm{Ct–}\varphi \rangle_{\mathrm{obs.}}$ (Å)	Ideal composition (*apfu*)
		Jinshajiangite, $Z = 4$			
$M^O(1)$	12.2(1)			2.166	
$M^O(2)$	12.5(1)			2.207	
$M^O(3)$	25.0(1)	$\mathrm{Fe^{2+}_{2.83}Mn_{0.63}Fe^{3+}_{0.31}Mg_{0.10}Zr_{0.04}\square_{0.09}}$		2.176	
$M^O(4)$	24.5(1)			2.185	
$M^O(5)$	25.2(2)			2.189	
ΣM^O	99.4		100.19		$\mathrm{Fe^{2+}_4}$
$M^H(1)$	22.4(1)	$\mathrm{Ti_{1.99}Nb_{0.01}}$		1.969	
$M^H(2)$	22.4(1)			1.964	
ΣM^H	44.8		44.19		$\mathrm{Ti_2}$
$^{[10]}A^P(1)$	26.25(8)	$\mathrm{Ba_{0.46}\square_{0.04}}$	25.76	2.901	
$^{[13]}A^P(2)$	17.5(1)	$\mathrm{K_{0.36}Ba_{0.12}\square_{0.52}}$	13.56	3.240	
ΣA^P	43.75	$\mathrm{Ba_{0.58}K_{0.36}\square_{0.06}}$	39.32		Ba
$^{[10]}B(1)$	6.60(8)	$\mathrm{Na_{0.32}Ca_{0.18}}$	7.12	2.624	$\mathrm{Na_{0.5}}$
$^{[10]}B(2)$	6.57(8)	$\mathrm{Na_{0.32}Ca_{0.18}}$	7.12	2.633	$\mathrm{Na_{0.5}}$
ΣB	13.17	$\mathrm{Na_{0.64}Ca_{0.36}}$	14.24		Na
$(^{[3]}X^O_{\mathrm{A}})_2$		$\mathrm{(OH)_{1.94}F_{0.06}}$			$\mathrm{(OH)_2}$
X^P_{M}		$\mathrm{F_{1.0}}$			F
		Surkhobite, $Z = 4$			
$M^O(1)$	12.40(8)			2.178	
$M^O(2)$	12.53(9)			2.219	
$M^O(3)$	25.1(1)	$\mathrm{Mn_{1.83}Fe^{2+}_{1.77}Fe^{3+}_{0.24}Mg_{0.03}Al_{0.03}\square_{0.10}}$		2.188	
$M^O(4)$	25.0(1)			2.195	
$M^O(5)$	25.4(2)			2.197	
ΣM^O	100.43		98.76		$\mathrm{Mn_4}$
$M^H(1)$	22.9(1)	$\mathrm{Ti_{1.82}Nb_{0.10}Zr_{0.08}}$		1.969	
$M^H(2)$	22.6(1)			1.966	
ΣM^H	45.5		47.42		$\mathrm{Ti_2}$
$^{[10]}A^P(1)$	27.15(8)	$\mathrm{Ba_{0.49}Sr_{0.01}}$	27.82	2.912	
$^{[13]}A^P(2)$	14.92(9)	$\mathrm{K_{0.38}Ba_{0.10}Cs_{0.02}\square_{0.50}}$	13.92	3.251	
ΣA^P	42.07	$\mathrm{Ba_{0.59}K_{0.38}Cs_{0.02}Sr_{0.01}}$	41.74		Ba
$^{[10]}B(1)$	7.12(6)	$\mathrm{Na_{0.30}Ca_{0.19}\square_{0.01}}$	7.10	2.627	$\mathrm{Na_{0.5}}$
$^{[10]}B(2)$	7.19(6)	$\mathrm{Na_{0.29}Ca_{0.20}\square_{0.01}}$	7.19	2.624	$\mathrm{Na_{0.5}}$
ΣB	14.31	$\mathrm{Na_{0.59}Ca_{0.39}\square_{0.02}}$	14.29		Na
$(^{[3]}X^O_{\mathrm{A}})_2$		$\mathrm{(OH)_{1.79}F_{0.21}}$			$\mathrm{(OH)_2}$
X^P_{M}		$\mathrm{F_{1.0}}$			F

gite and surkhobite. In bobshannonite, Ba occurs only at the $A^P(1)$ site, $\mathrm{Ba_{0.95}\square_{0.05}}$ *pfu*, and there is no Ba at the $A^P(2)$ site which is occupied mainly by K, $\mathrm{K_{0.93}Rb_{0.07}\square_{1.00}}$ *pfu*. Therefore, for bobshannonite, instead of writing an ideal composition of the two A^P sites as Ba *apfu* (see above for jinshajiangite and surkhobite), we write the ideal compositions of the two sites, $A^P(1)$ and $A^P(2)$, as BaK *apfu* ($Z = 2$).

The $B^P(1,2)$ sites are occupied by Na and Ca, where Na $>$ Ca (jinshajiangite, surkhobite) and solely Na plus minor vacancy (bobshannonite) (Table 6). The $B^P(1,2)$ sites are coordinated by eight O atoms and two F atoms at the X^P_{M} sites (jinshajiangite, surkhobite) (Fig. 2e) and by eight O atoms and two $\mathrm{X}^P_{\mathrm{M}}$ anions (bobshannonite, see above on occurrence of O and F atoms at the X^P_{M} site), with mean distances of 2.629 Å (jinshajiangite), 2.626 Å (surkhobite), and 2.656 Å (bobshannonite) (Tables 5, 6). There is no order of Na and Ca at the $B^P(1,2)$ sites in jinshajiangite and surkhobite; refined site-scattering values at the $B^P(1)$

TABLE 6. CONTINUED.

Site*	Refined site-scattering (*epfu*)	Assigned site-population (*pfu*)	Calculated site-scattering (*epfu*)	$<$Ct–φ$>_{obs.}$ (Å)	Ideal composition (*apfu*)
		Bobshannonite, $Z = 2$			
$M^{O}(1)$	25.8(1)			2.193	
$M^{O}(2)$	25.6(1)			2.242	
$M^{O}(3)$	47.3(1)	$Mn_{6.85}Fe^{2+}_{0.23}Zn_{0.23}Mg_{0.03}Al_{0.02}Zr_{0.04}Na_{0.52}\square_{0.12}$		2.202	
$M^{O}(4)$	46.7(1)			2.226	
$M^{O}(5)$	48.6(2)			2.298	
ΣM^{O}	194.0		192.07		(Mn_7Na)
$M^{H}(1)$	70.6(1)	$Nb_{2.73}Ti_{1.27}$		1.972	
$M^{H}(2)$	70.8(1)			1.973	
ΣM^{H}	141.4		139.87		Nb_4
$^{[10]}A^{P}(1)$	54.30(9)	$Ba_{0.95}\square_{0.05}$	53.20	2.922	Ba
$^{[13]}A^{P}(2)$	22.4(1)	$K_{0.93}Rb_{0.07}\square_{1.00}$	20.26	3.276	K
ΣA^{P}	76.70	$Ba_{0.95}\square_{0.05}\ K_{0.93}Rb_{0.07}\square_{1.00}$	73.46		Ba K
$^{[10]}B(1)$	10.77(7)	$Na_{0.95}\square_{0.05}$	10.45	2.656	Na
$^{[10]}B(2)$	10.75(7)	$Na_{0.94}\square_{0.06}$	10.34	2.656	Na
ΣB	21.52		20.79		Na_2
$(^{[3]}X^{O}_{A})_4$		$(OH)_4$			$(OH)_4$
X^{P}_{M}		$O_{1.32}F_{0.68}$			O_2

* Coordination numbers are shown for non-[6]-coordinated cations and non-[4]-coordinated anions; Ct – cation; φ – unspecified anion.

TABLE 7. BOND-VALENCE VALUES* FOR SELECTED ANIONS IN THE PERRAULTITE-TYPE MINERALS, SPACE GROUP $C\bar{1}$

Atom**	$M^{O}(1)$	$M^{O}(2)$	$M^{O}(3)$	$M^{O}(4)$	$M^{O}(5)$	$M^{H}(1)$	$M^{H}(2)$	$A^{P}(1)$	$A^{P}(2)$	$B^{P}(1)$	$B^{P}(1)$	Σ
						jinshajiangite						
$X^{O}_{M}(1)$	0.37		0.39		0.16	1.01						1.93
$X^{O}_{M}(2)$		0.16		0.37	0.27		1.05					1.85
$^{[3]}X^{O}_{A}(1)$	0.36			0.38	0.38							1.12
$^{[3]}X^{O}_{A}(2)$		0.35	0.42		0.35							1.12
$^{[6]}X^{P}_{M}$						0.31	0.32	0.11	0.07	0.09	0.09	0.99
						surkhobite						
$X^{O}_{M}(1)$	0.30		0.41		0.17	1.00						1.88
$X^{O}_{M}(2)$		0.17		0.38	0.29		1.02					1.86
$^{[3]}X^{O}_{A}(1)$	0.39			0.40	0.40							1.19
$^{[3]}X^{O}_{A}(2)$		0.39	0.43		0.38							1.20
$^{[6]}X^{P}_{M}$						0.33	0.33	0.11	0.06	0.09	0.09	1.01
						bobshannonite						
$X^{O}_{M}(1)$	0.27		0.36		0.15	1.10						1.88
$X^{O}_{M}(2)$		0.15		0.35	0.28		1.09					1.87
$^{[3]}X^{O}_{A}(1)$	0.39			0.37	0.39							1.15
$^{[3]}X^{O}_{A}(2)$		0.39	0.38		0.36							1.13
$^{[6]}X^{P}_{M}$						0.79	0.80	0.11	0.03	0.11	0.11	1.95

* Bond-valence parameters (*vu*) are from Brown (1981); $M^{O}(1–5) = Fe^{2+}$ (jinshajiangite) and Mn (bobshannonite, surkhobite); $M^{H}(1, 2) = Ti$ (jinshajiangite, surkhobite) and Nb (bobshannonite); $A^{P}(1) = Ba$; $A^{P}(2) = K$; $B^{P}(1, 2) = Na$; $^{[6]}X^{P}_{M} = F$ (jinshajiangite, surkhobite) and O (bobshannonite); $X^{O}_{M}(1, 2) = O$; $X^{O}_{A}(1,2) = OH$.

** Coordination numbers are shown for non-[4]-coordinated anions.

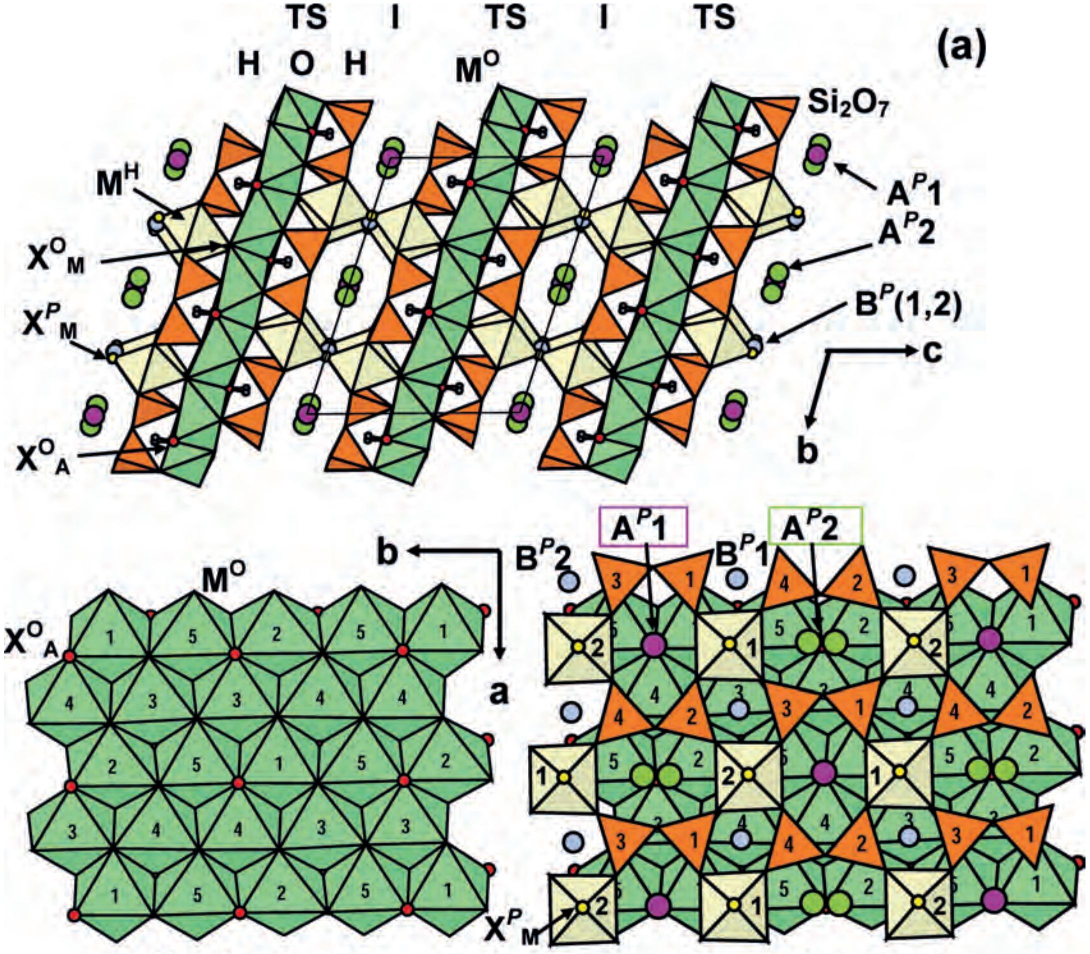

(b) O sheet

(c) O + H sheets

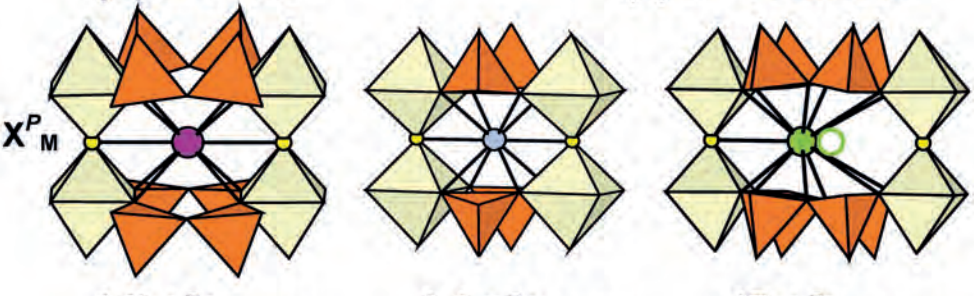

(d) A^{P}1 cage (e) B^{P}1 cage (f) A^{P}2 cage

FIG. 2. A general view of the crystal structure of jinshajiangite, a perraultite-type mineral, which consists of TS and **I** blocks (a) and the details of the TS block: the close-packed O sheet of Fe^{2+}-dominant M^O octahedra (b); the H sheet of Ti-dominant M^H octahedra and Si$_2$O$_7$ groups with the **I** block of Ba, K, and Na atoms at the $A^P(1)$, $A^P(2)$, and $B^P(1,2)$ sites superimposed on the O sheet (c); the A^P(1) cage with [10]-coordinated A^P(1) atom (d); the B^P(1) cage with [10]-coordinated B^P(1) atom (e); and the A^P(2) cage with the [13]-coordinated A^P(2) atom at one point of the $A^P(2)$ site–the position of a vacant point of the $A^P(2)$ site is shown by a white circle with a green rim (f). SiO$_4$ tetrahedra are orange, Ti- and Fe^{2+}-dominant octahedra

TABLE 8. HYDROGEN BONDING IN THE PERRAULTITE-TYPE MINERALS, SPACE GROUP $C\bar{1}$

D–H···A	D–H (Å)	H···A (Å)	D···A (Å)	∠ DHA (°)
		Jinshajiangite		
$X^O_A(1)$OH–H(1)···O(7)	0.98(1)	2.71(7)	3.29(1)	119(6)
$X^O_A(1)$OH–H(1)···O(8)	0.98(1)	2.54(6)	3.35(1)	140(7)
$X^O_A(2)$OH–H(2)···O(9)	0.98(1)	2.44(6)	3.041(6)	120(5)
$X^O_A(2)$OH–H(2)···O(10)	0.98(1)	2.45(7)	3.019(6)	117(5)
		Surkhobite		
$X^O_A(1)$OH–H(1)···O(7)	0.97(1)	2.56(4)	3.298(5)	132(3)
$X^O_A(1)$OH–H(1)···O(8)	0.97(1)	2.52(3)	3.340(5)	142(4)
$X^O_A(2)$OH–H(2)···O(9)	0.98(1)	2.41(4)	3.046(4)	123(3)
$X^O_A(2)$OH–H(2)···O(10)	0.98(1)	2.47(4)	3.014(4)	115(3)
		Bobshannonite		
$X^O_A(1)$OH–H(1)···O(7)	0.96(1)	2.51(2)	3.285(3)	137(2)
$X^O_A(1)$OH–H(1)···O(8)	0.96(1)	2.61(2)	3.353(3)	134(2)
$X^O_A(2)$OH–H(2)···O(9)	0.98(1)	2.60(3)	3.096(2)	111(2)
$X^O_A(2)$OH–H(2)···O(10)	0.98(1)	2.39(3)	3.046(2)	124(2)

and $B^P(2)$ sites are 6.60(9) and 6.57(8) *epfu* in jinshajiangite and 7.12(6) and 7.19(6) *epfu* in surkhobite. The ideal compositions of the $B^P(1)$ and $B^P(2)$ sites are $Na_{0.5}$ and $Na_{0.5}$ *apfu,* respectively (jinshajiangite, surkhobite, Z = 4) and $Na_{1.0}$ and $Na_{1.0}$ (bobshannonite, $Z = 2$). The ideal composition of the $B^P(1)$ + $B^P(2)$ sites is $Na_{1.0}$ *apfu* (jinshajiangite, surkhobite, $Z = 4$) and $Na_{2.0}$ *apfu* (bobshannonite, $Z = 2$).

We write the cation part of the structural formula of jinshajiangite and surkhobite as the sum of the following cations: (a) NaBa (B^PA^P) + (b) Fe^{2+}_4 [(M^O_4) (jinshajiangite)] and Mn_4 [(M^O_4) (surkhobite)] + (c) Ti_2 (M^H_2); ideally $NaBaFe^{2+}_4Ti_2$ (jinshajiangite, $Z = 4$) and $NaBaMn_4Ti_2$ (surkhobite, $Z = 4$), with a total charge of 19+. For bobshannonite, the cation part of the structural formula is the sum of the following cations: (a) Na_2KBa ($B^P_2A^P_2$); (b) (Mn_7Na) (M^O_8); (c) Nb_4 (M^H_4); ideally $Na_2KBa(Mn_7Na)Nb_4$ ($Z = 2$), with a total charge of 40+.

There are 14 anions, O(1–14) (Table 4), that coordinate the Si atoms and hence they are O atoms. Two $X^O_M(1,2)$ anions are ligands of three M^O cations and an M^H cation (Table 5) and they are O atoms, with bond-valence sums from 1.85 to 1.93 *vu* (valence units) (Table 7). Two $X^O_M(1,2)$ sites ideally give O_2 *pfu* (jinshajiangite, surkhobite, $Z = 4$) and O_4 *pfu* (bobshannonite, $Z = 2$). The $X^O_A(1,2)$ sites are occupied by $[(OH)_{1.94}F_{0.06}]$ *pfu* (jinshajiangite, $Z = 4$); $[(OH)_{1.79}F_{0.21}]$ *pfu* (surkhobite, $Z = 4$); and $(OH)_4$ *pfu* (bobshannonite, $Z = 2$) (Tables 2, 6). Therefore, the $X^O_A(1,2)$ sites are occupied mainly by O atoms of OH groups (Table 6), with bond-valence sums of 1.12–1.20 *vu* (Table 7). The H(1,2) atoms are involved in weak hydrogen bonds with O atoms that coordinate the polyhedra of the H sheets (Table 8). Two $X^O_A(1,2)$ sites ideally give $(OH)_2$ *pfu* (jinshajiangite, surkhobite, $Z = 4$) and $(OH)_4$ *pfu* (bobshannonite, $Z = 2$). The X^P_M anion is a bridging anion for two M^H atoms (Ti or Nb) and two B^P atoms (Na > Ca or solely Na); the X^P_M anion is bonded to one Ba atom [$A^P(1)$ site] and one $A^P(2)$ atom [either Ba or K at the $A^P(2)$ site] (Fig. 2a, c–f). Hence the coordination number of the X^P_M anion is 6. In jinshajiangite and surkhobite, the occurrence of F at the X^P_M site is in accord with the bond-valence sums of 0.99 and 1.01 *vu* at an X^P_M anion (Table 7). In bobshannonite, the X^P_M site is occupied by $O_{1.32}F_{0.68}$ *pfu*, in accord with the composition of the M^H site: $Nb_{2.73}Ti_{1.27}$ *apfu* (Table 6). The ideal composition of the X^P_M site is F *apfu* (jinshajiangite and surkhobite, $Z = 4$) and O_2 *apfu* (bobshannonite, $Z = 2$).

We write the anion part of the formulae of jinshajiangite and surkhobite as the sum of the

---

←

FIG. 2. (continued) are pale yellow and green; labels 1–5 on green correspond to $M^O(1–5)$ octahedra (b, c); labels 1 and 2 on pale yellow correspond to $M^H(1,2)$ octahedra; and labels 1–4 on orange correspond to Si(1–4) tetrahedra (c); Ba and K atoms at the A^P sites and Na atoms at the B^P sites in the **I** block are shown as large raspberry and green spheres and medium navy blue spheres; O and H atoms of OH groups at the X^O_A sites are shown as red and small grey spheres and O–H bonds are shown as black lines (a); F atoms at the X^P_M sites are shown as yellow spheres. Unit cell is shown by thin black lines in (a).

TABLE 9. IDEAL STRUCTURAL FORMULAE OF THE PERRAULTITE-TYPE MINERALS (STRUCTURE TYPE B1BG)*

	Ideal structural formula								
Mineral	A^P	B^P	$M^O{}_4$	$M^H{}_2$	$(Si_2O_7)_2$	$(X^O{}_M)_2$	$(X^O{}_A)_2$	$X^P{}_M$	Z
Perraultite	Ba	Na	Mn_4	Ti_2	$(Si_2O_7)_2$	O_2	$(OH)_2$	F	4
Surkhobite	Ba	Na	Mn_4	Ti_2	$(Si_2O_7)_2$	O_2	$(OH)_2$	F	4
Jinshajiangite	Ba	Na	$Fe^{2+}{}_4$	Ti_2	$(Si_2O_7)_2$	O_2	$(OH)_2$	F	4
Bobshannonite	KBa	Na_2	(Mn_7Na)	Nb_4	$(Si_2O_7)_4$	O_4	$(OH)_4$	O_2	2

* Formulae of perraltite and jinshajiangite are in accord with the current nomenclature of the seidozerite supergroup (Sokolova & Cámara 2017); formulae of surkhobite and bobshannonite have been revised.

following anions: $(Si_2O_7)_2$ + O_2 $(X^O{}_M)_2$ + $(OH)_2$ $(X^O{}_A)_2$ + F $(X^P{}_M)$, ideally $(Si_2O_7)_2O_2(OH)_2F$, $Z = 4$, with a total charge of 19–. The anion part of the formula of bobshannonite is written in the same way: $(Si_2O_7)_4$ + O_4 $(X^O{}_M)_4$ + $(OH)_4$ $(X^O{}_A)_4$ + O_2 $(X^P{}_M)_2$, ideally $(Si_2O_7)_4O_4(OH)_4O_2$, $Z = 2$, with a total charge of 40–.

In accord with the perraultite-type general formula, $B^PA^PM^O{}_4M^H{}_2(Si_2O_7)_2X^O{}_4X^P{}_M$ (Sokolova 2006), we write the ideal structural formulae of jinshajiangite, surkhobite, and bobshannonite as $NaBaFe^{2+}{}_4Ti_2(Si_2O_7)_2O_2(OH)_2F$, $Z = 4$; $NaBaMn_4Ti_2(Si_2O_7)_2O_2(OH)_2F$, $Z = 4$; and $Na_2KBa(Mn_7Na)Nb_4(Si_2O_7)_4O_4(OH)_4O_2$, $Z = 2$ (Table 9).

Interpretation of the IR Spectra

Previous work (*e.g.*, Cámara *et al.* 2016b) shows that in the jinshajiangite structure, F mainly occurs at the $X^P{}_M$ site in the H sheet and minor F occurs at the $X^O{}_A$ sites of the O sheet, whereas OH is ordered at the $X^O{}_A$ sites of the O sheet. The O (donor anion) in the O sheet is bonded to three M^O cations (Fig. 2b) and the O–H bond is directed toward Ba or K at the A^P site located above the hexagonal A^P ring of four Si tetrahedra and two Ti-dominant M^H octahedra (Fig. 2a, c). The geometry of the hydrogen bond for the refined jinshajiangite is given in Table 8, where D····A distances are in the range ~3.02 to 3.35 Å. From the empirical O···O bond distance *versus* wavenumber relation of Libowitzky (1999), the calculated absorption values are in the range 3600–3550 cm^{-1}, in close accord with the experimental data given here. The local configuration of the O–H group in jinshajiangite may be expressed as $M^OM^OM^O$–OH → A^P(Ba,K) where $M^O = Fe^{2+}$, Mn. Considering that there is no preferential order of Fe^{2+} and Mn at the $^{[6]}M^O$ sites of the O sheet, the statistical distribution of two cations over three available sites generates four arrangements (Hawthorne & Della Ventura 2007) and thus four peaks in the infrared spectrum. A tentative decomposition of the spectrum in Figure 1a by fitting Gaussian components to the experimental envelope (*e.g.*, Della Ventura *et al.* 1999, Della Ventura 2017) requires a minimum of four bands to reproduce the main absorption, neglecting for the moment the lower frequency absorption at 3497 cm^{-1} (Fig. 1b). There are two main points to consider in assigning the fitted components: (1) the studied sample contains Fe^{2+} >> Mn at the M^O sites, in addition to minor Fe^{3+}, Mg, and Zr (Table 6), hence only local Fe-rich configurations, *e.g.*, FeFeFe–OH or FeFeMn–OH, are expected to give visible bands in the spectrum; (2) in contrast to micas and amphiboles, there are two cations with different charge at the A^P sites (Ba^{2+} and K^+). The situation is somewhat analogous to that in tremolite and richterite in which the O–H bond points toward □ and Na, respectively, at the *A* site (Hawthorne & Della Ventura 2007). The charge difference of 1^+ at the *A* site causes a difference in absorption frequency of 55 cm^{-1} with the higher charge associated with the higher frequency. Using the similarity of local atomic arrangement around the OH group in the jinshajiangite and amphibole structures, one expects the absorption frequency in jinshajiangite to be ~55 cm^{-1} higher when the local arrangement involves Ba at the $A^P(1)$ site (Fig. 2d) rather than K at the $A^P(2)$ site (Fig. 2f). Using this information, it is therefore difficult to assign with confidence the observed bands to exact local configurations. A possible interpretation involves assignment of the first two peaks at 3632 and 3609 cm^{-1}, respectively, to the FeFeFe–OH and FeFeMn–OH arrangements facing the $A^P(1)$ cage occupied by Ba (Fig. 2d), while the next doublet at 3587 and 3559 cm^{-1}, is assigned to the same arrangements facing the $A^P(2)$ cage filled by (Ba, K) (Fig. 2f). The larger bandwidth of the lower-frequency doublet is in accord with the disorder at the $A^P(2)$ site. In addition, the Fe^{2+} *apfu* (2.73) from the intensity ratio of the fitted bands is in agreement with the Fe^{2+} assigned to the M^O sites (2.83, Table 6).

Crystal Chemistry of Perraultite-Type Minerals

Our structure-refinement results for triclinic jinshajiangite, surkhobite, and bobshannonite are in accord with the recent structure work on jinshajiangite by Jin *et al*. (2018), except for two new features: (1) the coordination number of the $A^P(2)$ cation is [13] compared to [9] reported by Jin *et al*. (2018) and (2) the H(1,2) atoms were included in the refinement and geometry of the hydrogen bonding has been established.

Sokolova & Cámara (2013) assigned structure type B1BG (B – basic, BG – bafertisite group) to the perraultite-type structure. The general topology of the perraultite-type structure (Jin *et al*. 2018) confirms the latter assignment and agrees with the definition of the basic structure by Sokolova & Cámara (2013): "A basic structure has the following four characteristics: In the basic structure, (1) There is only one type of TS block; (2) The two H sheets of the TS block are identical; (3) There is only one type of **I** block or it is absent; (4) There is only one type of self-linkage of TS blocks." Cámaraite, ideally $NaBa_3Fe^{2+}{}_8Ti_4(Si_2O_7)_4O_4(OH)_4F_3$, has a derivative structure (space group $C\bar{1}$), with one type of TS block, two types of **I** block, and two types of self-linkage of TS blocks (Sokolova *et al*. 2009b, Cámara *et al*. 2009). The structure of cámaraite can be built of structural fragments of two minerals of the same group, jinshajiangite and bafertisite, ideally $Ba_2Fe^{2+}{}_4Ti_2(Si_2O_7)_2O_2(OH)_2F_2$ (Cámara *et al*. 2016a).

Doubling of the t_1 and t_2 translations in jinshajiangite, surkhobite, and bobshannonite is due to the distortion of the A^P rings of polyhedra in the H sheets (Sokolova & Cámara 2016, Cámara *et al*. 2016b).

The ideal formula of bobshannonite has been revised as follows: $Na_2KBa(Mn_7Na)Nb_4(Si_2O_7)_4O_4(OH)_4O_2$, $Z = 2$ [*cf*. previous ideal formula $Na_2KBa(Mn,Na)_8(Nb,Ti)_4(Si_2O_7)_4O_4(OH)_4(O,F)_2$, $Z = 2$, Sokolova *et al*. (2015)].

On surkhobite

Based on our structure work on jinshajiangite and surkhobite, we write their ideal formulae as follows: jinshajiangite, $NaBaFe^{2+}{}_4Ti_2(Si_2O_7)_2O_2(OH)_2F$, $Z = 4$ [in accord with Sokolova (2006), Sokolova & Cámara (2017), and Jin *et al*. (2018)]; surkhobite, $NaBaMn_4Ti_2(Si_2O_7)_2O_2(OH)_2F$, $Z = 4$ [*cf*. current IMA formula $KBa_3Ca_2Na_2Mn_{16}Ti_8(Si_2O_7)_8O_8(OH)_4(F,O,OH)_8$, $Z = 2$]. In the introduction, we quoted Rastsvetaeva *et al*. (2008b) who redefined surkhobite as a "Mn-analogue of jinshajiangite and an ordered derivative of perraultite, with Ca ordered at one of the interstitial sites" in the **I** block. Above we showed that jinshajiangite and surkhobite are isostructural. However, there is no order of Na and Ca at the $B^P(1,2)$ sites in surkhobite (see structure description of surkhobite above).

Hence the definition of surkhobite as "an ordered derivative of perraultite, with Ca ordered at one of the interstitial sites" (Rastsvetaeva *et al*. 2008b) is not correct. It is obvious that surkhobite is not a valid mineral species: surkhobite and perraultite have the same formula, $NaBaMn_4Ti_2(Si_2O_7)_2O_2(OH)_2F$, $Z = 4$, perraultite was described by Chao (1991), surkhobite was reinstated by (Rastsvetaeva *et al*. 2008b) as a Ca-ordered derivative of perraultite; hence perraultite takes precedence over surkhobite, and surkhobite must be discredited.

We do not have perraultite from the Oktyabr'skii massif with which the crystal structure of perraultite was solved by Yamnova *et al*. (1998) and to which surkhobite was related by Rastsvetaeva *et al*. (2008b), but we are working in this direction. As soon as we refine the crystal structure of perraultite from the Oktyabr'skii massif using the structure model of Jin *et al*. (2018) and show that perraultite and surkhobite are isostructural, we will question of the validity of surkhobite as a mineral species in a formal manner.

Acknowledgments

We are grateful to reviewers Anthony R. Kampf and Marco E. Ciriotti and Associate Editor Jim Evans for very useful comments that improved the manuscript. We thank Professor Margarita Novgorodova, a former Director of the Fersman Mineralogical Museum, Moscow, for the loan of the holotype sample of surkhobite. This work was supported by a Discovery grant from the Natural Sciences and Engineering Research Council of Canada to FCH.

References

Brown, I.D. (1981) The bond valence method: an empirical approach to chemical structure and bonding. *In* Structure and Bonding in Crystals II (M. O'Keeffe & A. Navrotsky, eds.). Academic Press, New York, United States (1–30).

Cámara, F. & Sokolova, E. (2007) From structure topology to chemical composition. VI. Titanium silicates: The crystal structure and crystal chemistry of bornemanite, a group III Ti-disilicate mineral. *Mineralogical Magazine* **71**, 593–610.

Cámara, F. & Sokolova, E. (2009) From structure topology to chemical composition. X. Titanium silicates: The crystal structure and crystal chemistry of nechelyustovite, a group III Ti-disilicate mineral. *Mineralogical Magazine* **73**, 887–897.

Cámara, F., Sokolova, E., & Nieto, F. (2009) Cámaraite, $Ba_3NaTi_4(Fe^{2+},Mn)_8(Si_2O_7)_4O_4(OH,F)_7$. II. The crystal structure and crystal chemistry of a new group-II Ti-disilicate mineral. *Mineralogical Magazine* **73**, 855–870.

Cámara, F., Sokolova, E., & Hawthorne, F.C. (2012) Kazanskyite, $\mathrm{Ba\square TiNbNa_3Ti(Si_2O_7)_2O_2(OH)_2(H_2O)_4}$, a Group-III Ti-disilicate mineral from the Khibiny alkaline massif, Kola Peninsula, Russia: Description and crystal structure. *Mineralogical Magazine* **76**, 473–492.

Cámara, F., Sokolova, E., Abdu, Y.A., & Hawthorne, F.C. (2014) Saamite, $\mathrm{Ba\square TiNbNa_3Ti(Si_2O_7)_2O_2(OH)_2(H_2O)_2}$, a Group-III Ti-disilicate mineral from the Khibiny alkaline massif, Kola Peninsula, Russia: Description and crystal structure. *Canadian Mineralogist* **52**, 745–761.

Cámara, F., Sokolova, E., Abdu, Y.A., & Pautov, L.A. (2016a) From structure topology to chemical composition. XIX. Titanium silicates: Revision of the crystal structure and chemical formula of bafertisite, $\mathrm{Ba_2Fe^{2+}{}_4Ti_2(Si_2O_7)_2O_2(OH)_2F_2}$, a Group-II TS-block mineral. *Canadian Mineralogist* **54**, 49–63.

Cámara, F., Sokolova, E., & Hawthorne, F.C. (2016b) From structure topology to chemical composition. XXII. Titanium silicates: Revision of the crystal structure of jinshajiangite, $\mathrm{NaBaFe^{2+}{}_4Ti_2(Si_2O_7)_2O_2(OH)_2F}$, a Group-II TS-block mineral. *Canadian Mineralogist* **54**, 1187–1204.

Chao, G.Y. (1991) Perraultite, a new hydrous Na-K-Ba-Mn-Ti-Nb silicate species from Mont Saint-Hilaire, Québec. *Canadian Mineralogist* **29**, 355–358.

Della Ventura, G. (2017) The analysis of asbestos minerals using vibrational spectroscopies (FTIR, Raman): Crystal-chemistry, identification and environmental applications. *European Mineralogical Union Notes in Mineralogy* **18**, 135–169.

Della Ventura, G., Hawthorne, F.C., Robert, J.-L., Delbove, F., Welch, M.D., & Raudsepp, M. (1999) Short-range order of cations in synthetic amphiboles along the richterite-pargasite join. *European Journal of Mineralogy* **11**, 79–94.

Eskova, E.M., Dusmatov, V.D., Rastsvetaeva, R.K., Chukanov, N.V., & Voronkov, A.A. (2003) Surkhobite $\mathrm{(Ca,Na)(Ba,K)(Fe^{3+},Mn)_4Ti_2(Si_4O_{14})O_2(F,OH,O)_3}$. The new mineral (The Alai Ridge, Tadjkistan). *Zapiski Vserossijskogo Mineralogicheskogo Obchshestva* **132**(2), 60–67 (in Russian).

Filina, M.I., Aksenov, S.M., Sorokhtina, N.V., Chukanov, N.V., Kononkova, N.N., Belakovskiy, D.I., Britvin, S.N., Kogarko, L.N., Chervonnyi, A.D., & Rastsvetaeva, R.K. (2019) The new mineral fluorbarytolamprophyllite, $\mathrm{(Ba,Sr,K)_2[(Na,Fe^{2+})_3TiF_2][Ti_2(Si_2O_7)_2O_2]}$ and chemical evolution of lamprophyllite-group minerals in agpaitic syenites of the Kola Peninsula. *Mineralogy and Petrology* **113**, 533–553.

Hawthorne, F.C. & Della Ventura, G. (2007) Short-range order in amphiboles. *Reviews in Mineralogy and Geochemistry* **67**, 173–222.

Hong, W. & Fu, P. (1982) Jinshajiangite, a new Ba-Mn-Fe-Ti-bearing silicate mineral. *Geochemistry (China)* **1**, 458–464.

Jin, S., Xu, H., Lee, S., & Fu, P. (2018) Jinshajiangite: Structure, twinning and pseudosymmetry. *Acta Crystallographica* **B74**, 525–336.

Khomyakov, A.P., Men'shikov, Yu.P., Ferraris, G., Nèmeth, P., & Nechelyustov, G.N. (2005) Bykovaite, $\mathrm{BaNa\{(Na,Ti)_4[(Ti,Nb)_2(OH,O)_3Si_4O_{14}](OH,F)_2\}}$ $\mathrm{3H_2O}$ – the new heterophyllosilicate from Lovozero alkaline massif (Kola Peninsula, Russia). *Zapiski Rossiiskogo Mineralogicheskogo Obshchestva* **134**(5), 40–48 (in Russian).

Libowitzky, E. (1999) Correlation of O–H stretching frequencies and O–H···O hydrogen bond lengths in minerals. *Monatshefte für Chemie* **130**, 1047–1059.

Lykova, I.S., Pekov, I.V., Kononkova, N.N., & Shpanchenko, A.K. (2010) Jinshanjiangite and bafertisite from the Gremyakha-Vyrmes alkaline complex, Kola Peninsula. *Geology of Ore Deposits* **52**, 837–842.

Men'shikov, Yu.P., Bussen, I.V., Goiko, E.A., Zabavnikova, N.I., Mer'kov, A.N., & Khomyakov, A.P. (1975) Bornemanite - a new silicophosphate of sodium, titanium, niobium and barium. *Zapiski Vsesoyuznogo Mineralogicheskogo Obshchestva* **104**(3), 322–326 (in Russian).

Men'shikov, Yu.P., Khomyakov, A.P., Polezhaeva, L.I., & Rastsvetaeva, R.K. (1996) Shkatulkalite $\mathrm{Na_{10}MnTi_3Nb_3(Si_20_7)_6(OH)_2F\cdot 12H_2O}$ – a new mineral. *Zapiski Vserossiiskogo Mineralogicheskogo Obshchestva* **125**(1), 120–126 (in Russian).

Nèmeth, P., Khomyakov, A.P., Ferraris, G., & Men'shikov, Yu.P. (2009) Nechelyustovite, a new heterophyllosilicate mineral, and new data on bykovaite: A comparative TEM study. *European Journal of Mineralogy* **21**, 251–260.

Pakhomovsky, Ya.A., Panikorovskii, T.L., Yakovenchuk, V.N., Ivanyuk, G.Yu., Mikhailova, Ju.A., Krivovichev, S.V., & Bocharov, V.N. (2018) Selivanovaite, $\mathrm{NaTi_3(Ti,Na,Fe,Mn)_4(Si_2O_7)_2O_4(OH,H_2O)_4]\cdot \mathit{n}H_2O}$, a new rock-forming mineral from the eudialyte-rich malignite of the Lovozero alkaline massif (Kola Peninsula, Russia). *European Journal of Mineralogy* **30**, 525–535.

Pautov, L.A., Agakhanov, A.A., Karpenko, V.Yu., Uvarova, Yu.A., Sokolova, E., & Hawthorne, F.C. (2019) Rinkite-(Y), $\mathrm{Na_2Ca_4YTi(Si_2O_7)_2OF_3}$, a seidozerite-supergroup TS-block mineral from the Darai-Pioz alkaline massif, the Tien-Shan mountains, Tajikistan: Description and crystal structure. *Mineralogical Magazine* **83**, 373–380.

Pekov, I.V., Belovitskaya, Yu.V., Kartashov, P.M., Chukanov, N.V., Yamnova, N.A., & Egorov-Tismenko, Yu.K. (1999) The new data on perraultite (The Azov sea region). *Zapiski Vserossiskogo Mineralogicheskogo Obshchetstva* **128**(3), 112–120 (in Russian).

POUCHOU, J.L. & PICHOIR, F. (1985) "PAP" φ(ρZ) procedure for improved quantitative microanalysis. *In* Microbeam analysis (J.T. Armstrong, ed.). San Francisco Press, San Francisco, California, United States (104–106).

RASTSVETAEVA, R.K., CHUKANOV, N.V., & ROZENBERG, K.A. (2008a) Crystal structure of jinshajiangite from the Norra Kärr Complex (Sweden). *Crystallography Reports* **53**, 553–556.

RASTSVETAEVA, R.K., ESKOVA, E.M., DUSMATOV, V.D., CHUKANOV, N.V., & SCHNEIDER, F. (2008b) Surkhobite: Revalidation and redefinition with the new formula, $(Ba,K)_2CaNa(Mn,Fe^{2+},Fe^{3+})_8Ti_4(Si_2O_7)_4O_4(F,OH,O)_6$. *European Journal of Mineral*ogy **20**, 289–295.

ROZENBERG, K.A., RASTSVETAEVA, R.K., & VERIN, I.A. (2003) Crystal structure of surkhobite: New mineral from the family of titanosilicate micas. *Crystallography Reports* **48**, 384–389.

SHANNON, R.D. (1976) Revised effective ionic radii and systematic studies of interatomic distances in halides and chalcogenides. *Acta Crystallographica* **A32**, 751–767.

SHELDRICK, G.M. (2015) Crystal structure refinement with SHELX. *Acta Crystallographica* **C71**, 3–8.

SOKOLOVA, E. (2006) From structure topology to chemical composition. I. Structural hierarchy and stereochemistry in titanium disilicate minerals. *Canadian Mineralogist* **44**, 1273–1330.

SOKOLOVA, E. (2010) Predictive crystal-chemical relations in Ti-silicates based on the TS block. *Geology of Ore Deposits* **52**, 410–427.

SOKOLOVA, E. & CÁMARA, F. (2013) From structure topology to chemical composition. XVI. New developments in the crystal chemistry and prediction of new structure topologies for titanium disilicate minerals with the TS block. *Canadian Mineralogist* **51**, 861–891.

SOKOLOVA, E. & CÁMARA, F. (2016) From structure topology to chemical composition. XXI. Understanding the crystal chemistry of barium in TS-block minerals. *Canadian Mineralogist* **54**, 79–95.

SOKOLOVA, E. & CÁMARA, F. (2017) The seidozerite supergroup of TS-block minerals: nomenclature and classification, with change of the following names: rinkite to rinkite-(Ce), mosandrite to mosandrite-(Ce), hainite to hainite-(Y) and innelite-1*T* to innelite-1*A*. *Mineralogical Magazine* **81**, 1457–1484.

SOKOLOVA, E. & CÁMARA, F. (2018) From structure topology to chemical composition. XXV: New insights into the close packing of cations in the structures of the seidozerite-supergroup TS-block minerals. *Zeitschrift für Kristallographie* **233**(3–4), 205–221.

SOKOLOVA, E., CÁMARA, F., HAWTHORNE, F.C., & ABDU, Y. (2009a) From structure topology to chemical composition. VII. Titanium silicates: The crystal structure and crystal chemistry of jinshajiangite. *European Journal of Mineralogy* **21**, 871–883.

SOKOLOVA, E., ABDU, Y., HAWTHORNE, F.C., STEPANOV, A.V., BEKENOVA, G.K., & KOTEL'NIKOV, P.E. (2009b) Cámaraite, $Ba_3NaTi_4(Fe^{2+},Mn)_8(Si_2O_7)_4O_4(OH,F)_7$. I. A new titanium-silicate mineral from the Verkhnee Espe deposit, Akjailyautas Mountains, Kazakhstan. *Mineralogical Magazine* **73**, 847–854.

SOKOLOVA, E., CÁMARA, F., ABDU, Y.A., HAWTHORNE, F.C., HORVÁTH, L., & PFENNINGER-HORVÁTH, E. (2015) Bobshannonite, $Na_2KBa(Mn,Na)_8(Nb,Ti)_4(Si_2O_7)_4O_4(OH)_4(O,F)_2$, a new TS-block mineral from Mont Saint-Hilaire, Québec, Canada: Description and crystal structure. *Mineralogical Magazine* **79**, 1791–1811.

SOKOLOVA, E., CÁMARA, F., HAWTHORNE, F.C., & PAUTOV, L.A. (2016) From structure topology to chemical composition. XX. Titanium silicates: The crystal structure of hejtmanite, $Ba_2Mn_4Ti_2(Si_2O_7)_2O_2(OH)_2F_2$, a Group-II TS-block mineral. *Mineralogical Magazine* **80**, 841–853.

WILSON, A.J.C. (Ed.) (1992) *International Tables for Crystallography, Volume C: Mathematical, physical and chemical tables*. Kluwer Academic Publishers, Dordrecht, Netherlands.

YAMNOVA, N.A., EGOROV-TISMENKO, YU.K., & PEKOV, I.V. (1998) Crystal structure of perraultite from the coastal region of the Sea of Azov. *Crystallography Reports* **43**, 401–410.

ZOLOTAREV, A.A., JR., SELIVANOVA, E.A., KRIVOVICHEV, S.V., SAVCHENKO, Y.E., PANIKOROVSKII, T.L., LYALINA, L.M., PAUTOV, L.A., & YAKOVENCHUK, V.N. (2018) Shkatulkalite, a rare mineral from the Lovozero Massif, Kola Peninsula: A re-investigation. *Minerals* **8**, 303–314.

Received September 17, 2019. Revised manuscript accepted October 23, 2019.